


# Shear Strength of Initially Unsaturated Soil

Intermediate results measurements Oijen and Westervoort

POV

MACRO  
STABILITEIT



Date: December 2020  
Author: Alexander van Duinen

Versie: 3.0

**Title**

Shear Strength of Initially Unsaturated Soil

Client	Project	Attribute	Pages
Projectoverstijgende Verkenning Macrostabiliiteit (POVM)	11204453-002	11204453-002-GEO-0001	63

**Keywords**

Shear strength, unsaturated soil, volumetric water content, suction, cone penetration tests, field vane tests, laboratory tests




**Summary**

Commissioned by the Directorate-General for Public Works and Water Management and the Project Overstijgende Verkenning Macrostabiliiteit (POVM), Deltares is working on a study of the shear strength of (initially) unsaturated soil in relation to the assessment and design of slope stability of dykes. The purpose of this research is to prepare a guideline for the stability analysis of flood defence dykes, in which unsaturated conditions of low permeable soil layers play a role in determining the shear strength parameters. For this research field and laboratory tests take place at the IJsseldijk near Westervoort (Dp. 250 + 80) and at the Maasdijk near Oijen (Dp. 592 - 593). The approach for this research follows the results and recommendations of the research conducted in 2019 commissioned by Rijkswaterstaat (Deltares, 2019a). This report describes the methods and results of the monitoring of volumetric water content, suction and pore water pressure and the measurements of the in-situ shear strength with cone penetration tests and field vane tests and the laboratory tests. This report will grow during the course of the project. During the project new results will be added to the report.

This report has also been released under project number 11205262-010-GEO-0001 on behalf of Rijkswaterstaat (project Kennis voor Keringen).

**References**

2019111165/2019116989, September 18, 2019

Version	Date	Author	Initials	Review	Initials	Approval	Initials
1.0	Dec. 2019	T.A. van Duinen MSc		dr.ir. C. Zwanenburg		ir. L. Voogt	
2.0	March 2020	T.A. van Duinen MSc		dr.ir. C. Zwanenburg		ir. L. Voogt	
3.0	Dec. 2020	T.A. van Duinen MSc		dr.ir. C. Zwanenburg		Ing. G. de Vries	

**Status**

Final

## Content

<b>1</b>	<b>Introduction</b>	<b>8</b>
1.1	Background	8
1.2	Objective of the project	9
1.3	Approach	9
1.4	Outline	10
<b>2</b>	<b>Study areas</b>	<b>11</b>
2.1	IJsseldijk Westervoort	11
2.2	Maasdijk Oijen	11
<b>3</b>	<b>Methods</b>	<b>13</b>
3.1	Introduction	13
3.2	Volumetric water content measurements	16
3.3	Suction stress measurements	17
3.4	Pore water pressure measurements	19
3.5	Cone penetration tests	20
3.6	Resistivity Cone Penetration Tests (RCPT)	23
3.7	Field vane tests	24
3.8	Boreholes	27
3.9	Classification tests	27
3.10	Determination of shear strength in the laboratory	28
3.11	Proctor test	29
3.12	Determination of retention curves and shrinkage curves	29
3.13	Mercury intrusion porosimetry tests	30
<b>4</b>	<b>Results</b>	<b>31</b>
4.1	Introduction	31
4.2	Volumetric water content measurements	31
4.3	Suction stress measurements	33
4.4	Pore water pressure measurements	36
4.5	Cone penetration tests, field vane tests	38
4.6	Resistivity Cone Penetration Tests (RCPT)	43
4.7	Boreholes	44
4.8	Classification tests	44
4.9	Determination of shear strength in the laboratory	48
4.10	Proctor test	51
4.11	Determination of retention curves and shrinkage curves	51
4.12	Mercury intrusion porosimetry tests	52
<b>5</b>	<b>Summary</b>	<b>55</b>
<b>6</b>	<b>References</b>	<b>56</b>

## Appendices

A	Results of in situ tests and classification tests of location Westervoort (in Dutch)	59
B	Results of in situ tests and classification tests of location Oijen (in Dutch)	60
C	Results of laboratory tests on intact and reconstituted samples of locations Oijen and Westervoort	61
D	Results of triaxial tests and HYPROP tests on intact samples of locations Westervoort and Oijen	62
E	Results of mercury intrusion porosimetry (MIP) tests and determination of specific surface on intact samples of locations Westervoort and Oijen	63

## Figures

Figure 2.1	Measurement location at the IJsseldijk at Westervoort.	11
Figure 2.2	Measurement location at the Maasdijk at Oijen.	12
Figure 3.1	The cone resistance in unsaturated aggregated soil is overestimated in case of large distance between the cracks, and the $Nk$ value should therefore increase (Powell & Quarterman, 1988).	22
Figure 3.2	Effect of suction on normalized cone resistance, for soils with different plasticity index (Miller, Collins, Muraleetharan, Cerato, & Doumet, 2015). The cone resistance has been normalized using the total vertical overburden pressure.	23
Figure 3.3	Correction factor to adjust FVT measurements (Azzouz et al., 1983). The correction factor is based on back-analyses of failures. Be aware of the considerable uncertainty of the correction factor.	26
Figure 4.1	Measured volumetric water content at Westervoort at the outer toe.	31
Figure 4.2	Measured volumetric water content at Westervoort at the inner toe.	32
Figure 4.3	Measured volumetric water content at Westervoort at the inner berm.	32
Figure 4.4	Measured volumetric water content at Oijen.	33
Figure 4.5	Measured suction stress at Westervoort at the outer toe.	34
Figure 4.6	Measured suction stress at Westervoort at the inner toe.	34
Figure 4.7	Measured suction stress at Westervoort at the inner berm.	35
Figure 4.8	Measured suction stress at Oijen.	35
Figure 4.9	Measured piezometric head at Westervoort at the outer toe.	36
Figure 4.10	Measured piezometric head at Westervoort at the inner toe.	37
Figure 4.11	Measured piezometric head at Westervoort at the inner berm.	37
Figure 4.12	FVT and CPT (class 1) results of location Westervoort at four times during the measurement period.	38
Figure 4.13	CPT (class 1, even numbers) results of location Westervoort.	39
Figure 4.14	CPT (class 1, odd numbers) results of location Westervoort.	39
Figure 4.15	FVT and CPT (class 1) results of location Oijen.	41
Figure 4.16	CPT (class 1 odd numbers) results of location Oijen.	42
Figure 4.17	CPT (class 1 even numbers) results of location Oijen.	42
Figure 4.18	Comparison of the results of the electrical conductivity measurements from the RCPT and volumetric water content measurements from the sensors at Oijen (a) and Westervoort (b). A factor 130 is used for both sites to get a good comparison.	44
Figure 4.19	Profiles of (a) soil unit weight, (b) organic content (OC) and (c) specific gravity of the soil particles ( $G_s$ ) against depth from borehole B201 at Westervoort.	45
Figure 4.20	Profile of clay, silt and sand content against depth from borehole B201 at Westervoort.	45

Figure 4.21	Profiles of (a) plastic limit $w_p$ , liquid limit $w_L$ and gravimetric water content $w$ and (b) plasticity index $I_p$ against depth from borehole B201 at Westervoort.	46
Figure 4.22	Profiles of (a) soil unit weight, (b) organic content (OC) and (c) specific gravity of the soil particles ( $G_s$ ) against depth from borehole B001 at Oijen.	46
Figure 4.23	Profile of clay, silt and sand content against depth from borehole B001 at Oijen.	47
Figure 4.24	Profiles of (a) plastic limit $w_p$ , liquid limit $w_L$ and gravimetric water content $w$ and (b) plasticity index $I_p$ against depth from borehole B001 at Oijen.	47
Figure 4.25	Relationship between water content and shear strength as derived from UU triaxial compression tests on intact samples (tests are performed at TU Delft).	49
Figure 4.26	Results of the Proctor test.	51
Figure 4.27	Example of HYPROP test resulting in a soil water retention curve.	52
Figure 4.28	Example of shrinkage test.	52
Figure 4.29	Pore size distribution from six intact clay samples determined with mercury intrusion porosimetry.	54
Figure 4.30	Pore size distribution from six reconstituted clay samples determined with mercury intrusion porosimetry.	54

## Tables

Table 3.1	Performed CPTs, FVTs and boreholes at Westervoort.	14
Table 3.2	Performed CPTs, FVTs and boreholes at Oijen.	15
Table 3.3	Volumetric water content devices at IJsseldijk Westervoort. The indicated depth of the sensors is halfway the probe rods.	17
Table 3.4	Volumetric water content devices at Maasdijk Oijen. The indicated depth of the sensors is halfway the probe rods.	17
Table 3.5	Tensiometers at IJsseldijk Westervoort.	18
Table 3.6	Tensiometers at Maasdijk Oijen.	19
Table 3.7	Pore water measurement devices at IJsseldijk Westervoort.	19
Table 4.1	Specific surface of intact samples determined with N <sub>2</sub> BET method.	48
Table 4.2	Specific surface of reconstituted samples determined with N <sub>2</sub> BET method.	48
Table 4.3	Results of UU triaxial compression tests on intact samples.	48
Table 4.4	Results of direct simple shear (DSS) tests and direct shear (DS) tests on intact samples.	49
Table 4.5	Results of CIU triaxial compression tests on reconstituted samples which are moist compacted using a Proctor hammer and Proctor mould with different compaction effort.	50
Table 4.6	Results of CIU triaxial compression tests on reconstituted samples which are made from a slurry and dried to different target water contents.	50
Table 4.7	Results of oedometer tests.	51
Table 4.8	Intact clay samples for the determination of the pore size distribution.	53
Table 4.9	Reconstituted clay samples for the determination of the pore size distribution.	53

# 1 Introduction

## 1.1 Background

Commissioned by the Directorate-General for Public Works and Water Management and the Project Overstijgende Verkenning Macrostabieliteit (POVM), Deltares is working on a study of the shear strength of (initially) unsaturated soil in relation to the assessment and design of the slope stability of dykes. The purpose of this research is to prepare a guideline for the stability analysis of flood defence dykes, in which unsaturated conditions of low permeable soil layers play a role in determining the shear strength parameters. The present guidelines and regulations for stability assessment of water retaining structures in the Netherlands (WBI 2017; Ministerie van Infrastructuur en Milieu, 2019) assume fully saturated conditions during a high-water event for the different subsoil layers and the dyke body. For fully saturated low permeable soil layers the guidelines assume undrained soil behaviour. However, in practice some waterboards apply drained soil behaviour with the use of the friction angle  $\phi'$  for initially unsaturated soils, also for clayey soil layers. In order to come to a clear approach for water boards the development of a guideline for initially unsaturated soils is necessary. In the method, the shear strength must be interpreted on the basis of field and laboratory tests, taking into account the variations in moisture content and suction stress in the subsurface and the dyke material. From the normal daily unsaturated conditions, it must be possible to make a translation into the conditions at high water. This can be the fully saturated state or a state with a higher degree of saturation compared to normal daily conditions. The guideline should lead to more accurate analyses of the slope stability of dykes, both for assessments and design, which describe the soil behaviour well.

The research focusses on both, the unsaturated behaviour of the subsoil and the unsaturated behaviour of the dyke body itself. For eastern and south eastern part of the Netherlands, 'bovenrivierengebied', unsaturated conditions occur often. Here the Holocene layer is relatively thin with relatively low ground water tables. Questions were raised on the influence of the unsaturated soil behaviour in the strength development for these locations. The presence of an unsaturated zone in the dyke body is not typical for the conditions found in the eastern and south eastern part of the Netherlands. All around the country dyke bodies will have a partly saturated zone. However, for these areas, the influence of the unsaturated zone is believed to be small in most cases, considering the total length of a possible sliding plane and the length of the part of the sliding plane that runs through the unsaturated soil.

A complicating factor is the fluctuating water and groundwater tables near water retaining structures. Consequently, the degree of saturation of the cohesive soil in the embankment and in the upper part of the Holocene cover layer varies during the year. Due to moisturizing, evapotranspiration and seepage processes, this part of the soil can become fully saturated in the wet season, winter, and will be partially saturated in the dry season, summer. If the soil becomes partially saturated during the dry season, the shear strength will temporary increase along a certain height, because of capillary suction. Field work conducted for stability assessment is typically done in the summer, dry, period, while the results need to be applied for the winter, wet, period. This imposes questions on whether soil which is unsaturated in summer time becomes fully saturated in winter time and if cracks that are formed in the dry period, close during the wet period. Consequences of these seasonal effects are also found when interpreting cone penetration tests. The present guidelines prescribe an additional reduction of the net cone resistance of unsaturated soil with a factor 3, when relating it to



saturated undrained soil strength. This method is however not underpinned very solidly. The WBI 2017 regulations finally prescribe that the favourable effect of suction stress on the shear strength above the phreatic level belonging to high water levels must be ignored and that a fully drained strength should directly be assumed.

## 1.2 Objective of the project

The ultimate goal of this study is to supply guidance on the characterization of the shear strength in cohesive soils in dykes and Holocene cover layers that is assumed to be fully saturated for assessment and design conditions, wet season, but not fully saturated during the dry season when parameter assessment takes place. This objective follows the research in 2019 commissioned by Rijkswaterstaat (Deltares, 2019a).

An important question to be answered in this research in order to achieve the objectives is whether an initially unsaturated soil becomes fully saturated during a high-water event. This is usually assumed for assessments and design of flood defence dykes, since it is expected to be a safe assumption, but this needs to be verified to obtain insight in the real behaviour of initially unsaturated soils. Next question is if an initially unsaturated soil due to infiltration and saturation becomes as low permeable as required to behave undrained during a potential slope failure.

In order to reach the objectives and these two key questions, the following scientific questions were formulated:

1. What is the typical variation in moisture content of the cohesive soil in the dykes and the cover layers, if not constantly saturated?
2. For which hydraulic conditions and soil properties the soil becomes completely saturated during the wet season, when the precipitation and evaporation are given?
3. To what extent do the macro-pores in aggregated soil close at the saturated state, as a result of swelling of the aggregates? And which factors are of influence?
4. What are suitable criteria regarding texture, moisture and aggregation to decide if the shear strength of saturated soil strength should be modelled drained or undrained, in case of stability analysis of primary flood defence dykes?
5. How does the moisture content and the coupled swelling and shrinkage behaviour affect the (drained or undrained) shear strength?
6. What is the relationship between the shear strength of the aggregates and the shear strength of the soil: to which extent can they be considered equal?

## 1.3 Approach

For this research field and laboratory tests take place at the IJsseldijk near Westervoort (dyke post Dp. 250 + 80) and at the Maasdijk near Oijen (dyke post Dp. 592 - 593). The approach for this research follows the results and recommendations of the research conducted in 2019 commissioned by Rijkswaterstaat (Deltares, 2019a). The approach is also described in the research proposals for Rijkswaterstaat (Deltares, 2019b) and the Projectoverstijgende Verkenning Macro stabiliteit (Deltares, 2019c). At both locations suction pressure meters (tensiometers) and volumetric water content sensors are installed in the (initially) unsaturated zone. At the IJsseldijk location, piezometers are installed in the saturated zone of the low permeable cover layer and the top of the aquifer. The measurements with these sensors will presumably be continued until the end of 2021. The aim is to get a good picture of the development of the volumetric water content, suction stress and water pressure during the various seasons and under the influence of precipitation, evaporation and the river water level.

Close to the sensors, cone penetration tests (CPTs), field vane tests (FVTs) and mechanical drillings with undisturbed sampling are carried out. This part of the field research is carried out by a contractor (Ingenieursbureau Wiertsema & Partners bv). The field tests are repeated with a certain regularity during the entire period in which the measurements are made with the sensors. This means that the tests are also conducted during the winter season (usually closed season for geotechnical investigations around dykes). These field tests will also be continued in 2021. Classification tests and other laboratory tests are performed on the soil samples. The classification tests are carried out by Wiertsema & Partners. Laboratory tests are conducted by Deltares, TU Delft and Delft Solids Solutions.

For the site investigations it is desirable to use CPTs with measurement of the dielectric constant or permittivity. At present there is no cone available in the market that meets the desired specifications. Wiertsema & Partners has a CPT cone with the possibility to measure the dielectric constant. This cone is tested in the laboratory of Deltares and in the field at Westervoort and Oijen.

#### **1.4 Outline**

This report describes the methods and results of the monitoring of volumetric water content, suction stress and pore water pressure and the measurements of the in-situ shear strength with cone penetration tests and field vane tests. This report will grow during the course of the project. During the project new results will be added to the next versions of this report. In the final stage of the project also the interpretation of the measurement results and conclusions of the research will be added.

Chapter 2 gives a short description of the two measurement sites IJsseldijk at Westervoort (Dp. 250 + 80) and Maasdijk at Oijen (Dp. 592 - 593). Chapter 3 describes the methods which are applied in the research. The sensors which measure volumetric water content, suction stress and pore water pressure and the in-situ tests to measure shear strength are described. For both sites also boreholes are carried out. For the Westervoort and Oijen location classification tests and laboratory tests are carried out on samples from the boreholes. The methods used to perform the boreholes, classification tests and the laboratory tests are also described in Chapter 3. In Chapter 4 the results of the measurements with the various sensors and the results of the in-situ tests, boreholes, classification tests and laboratory tests are presented. Chapter 5 gives a brief summary of the report.

This report has also been released under project number 11205262-010-GEO-0001 on behalf of Rijkswaterstaat (project Kennis voor Keringen).

## 2 Study areas

### 2.1 IJsseldijk Westervoort

The measurement site Westervoort is situated at the IJsseldijk (dyke post Dp. 250 + 80) northwestward of the village Westervoort (see Figure 2.1). The IJsseldijk is part of the administration of Waterboard Rijn en IJssel.

A floodplain lies between the dyke and the river IJssel. The width of the floodplain is about 250 m. A large pond is situated in the floodplain. On the crest of the dyke is a road. At the inner site of the dyke is a berm with a grass-plot.

The in-situ measurements are carried out at the outer toe, crest, inner toe and on the inner berm. The sensors are installed at the outer toe, inner toe and on the inner berm. At the crest only one CPT is carried out. Details of the set-up of the in-situ measurements are given in Chapter 3.



Figure 2.1 Measurement location at the IJsseldijk at Westervoort

The subsoil at the IJsseldijk consist of about 4.0 m thick Holocene clayey layers and sandy clay layers. These clayey layers lie on top of the Pleistocene sand layer. This stratigraphy is derived from a geotechnical site investigation (Inpijn-Blokpoel, 2017), which is conducted for Waterboard Rijn en IJssel.

### 2.2 Maasdijk Oijen

At Oijen the measurement site is situated on the crest of the Maasdijk between the dyke posts Dp. 592 and Dp. 593 (see Figure 2.2). The official name of the dyke is Oijense Benedendijk. The Maasdijk is part of the administration of Waterboard Aa en Maas. The measurement site is located in the dyke section Ravenstein – Lith.

At this site also a floodplain is situated in front of the dyke. The width of the floodplain is about 380 m. Some channels and ponds are in the floodplain. The dyke is a relatively new

construction, as the dyke was built in the 50s of the last century, according to the topographic maps, which are available on the website [www.topotijdreis.nl](http://www.topotijdreis.nl). The old dyke lies up to 100 m behind the new dyke. The topographic maps show a small pond just in front of the old dyke in the period before 1890. This small pond may be filled with soil in later years and may be a reason for the settlement of the crest of the new dyke around the dyke posts Dp. 592 – 593. The area between the old dyke and the new dyke has been raised to the same height as the crest of the dykes.

The measurement location is on the crest of the dyke. At the crest of the dyke the sensors are installed and the CPTs and FVTs are performed. Details of the set-up of the in-situ measurements are given in Chapter 3.



Figure 2.2 Measurement location at the Maasdijk at Oijen

The subsoil at the Maasdijk consist of 1.0 to 3.0 m thick Holocene clay layers and sandy clay layers on top of the Pleistocene sand layer. The new dyke is built from clay and sandy clay. This information is derived from geotechnical profiles of the Maasdijk (Grondmechanica Delft, 1996).

## 3 Methods

### 3.1 Introduction

At the IJsseldijk location near Westervoort the research is carried out at the outer toe, crest, inner toe and inner berm. On the outer toe, crest, inner toe and on the inner berm, CPTus class 2 are carried out as a preliminary survey. At Westervoort some of the CPTus are applied with an additional magnetic module to trace potentially present explosives.

Suction stress sensors (tensiometers), volumetric water content sensors and pore water pressure sensors (piezometers) are installed at the outer toe, inner toe and at the inner berm. The tensiometers and the water content sensors are installed in the top of the clayey cover layer, between 1.0 and 2.5 m below surface level. The pore water pressure sensors are placed in the bottom of the clayey cover layer and in the top of the Pleistocene water-bearing sand layer (aquifer).

CPTs class 1 and FVTs to measure the shear strength of the soil are also carried out on the inner berm. The field investigation on the inner berm will be repeated with a regular interval during the entire measurement period. The goal of these measurements is to correlate volumetric water content, suction stress to shear strength to gain the understanding in the importance of the seasonal variation of volumetric water content and suction stress on the shear strength. Each time the CPTs and FVTs are performed double to be able to assess the heterogeneity of the shear strength.

At the Maasdijk near Oijen a similar approach is followed. At the Maasdijk the research is carried out only on the crest of the dyke. Here also CPTus class 2 are performed as a preliminary survey. The volumetric water content sensors and tensiometers are installed at the crest of the dyke at 1.0 to 3.1 m below surface level. Similar to Westervoort CPTs class 1 and FVTs are conducted to measure the shear strength of the soil. Piezometers are not applied in Oijen.

At Westervoort and Oijen also mechanical drillings are performed. The samples of the boreholes are used to perform classification tests, triaxial tests, direct shear tests, direct simple shear tests, oedometer tests and mercury intrusion porosimetry (MIP) tests in the laboratory.

Table 3.1 and Table 3.2 give an overview of the CPTs, FVTs and boreholes which are performed at Westervoort and Oijen up to now. The set-up of the site investigations at Westervoort and Oijen is given in Appendix A and Appendix B respectively. The field descriptions of the boreholes are also presented in Appendix A and Appendix B.

Date	CPT class 1 (DKM) or CPT class 1 with electric resistivity measurement (DKMG)	CPTu class 2 with magnetocone (DKM) or $u_2$ measurement (DKMP)	FVT	Borehole
23-10-2019		DKMP2003, DKMP2004, DKM2201, DKM2202, DKM2203		
24-10-2019		DKMP2001, DKMP2002, DKM2200		
31-10-2019	DKM2005, DKM2006		TV202	B201
Start of the monitoring of volumetric water content, suction stress and pore water pressure.				
1-11-2019			TV201	
15-11-2019	DKM2007, DKM2008			
28-11-2019	DKM2009			
29-11-2019	DKM2010		TV203	
19-12-2019	DKM2011, DKM2012			
13-1-2020	DKM2013, DKM2014			
4-2-2020	DKM2015, DKM2016			
10-2-2020	DKM2017, DKM2018			
10-3-2019	DKM2019, DKM2020			
6-4-2020	DKM2021, DKM2022		TV206 test 1	
7-4-2020			TV206 test 2-7 TV205 test 1-2	
8-4-2020			TV205 test 3-7	
11-5-2020	DKM2023, DKM2024			
5-6-2020	DKM2025, DKM2026			
29-6-2020	DKM2027, DKM2028			
21-7-2020	DKM2029, DKM2030			
11-8-2020				B202, B203
24-8-2020	DKM2031, DKM2032			
7-9-2020	DKM2033, DKM2034			
8-9-2020			TV207	
9-9-2020			TV208	
30-9-2020	DKMG2045, DKMG2046			
29-10-2020	DKM2035, DKM2036			
3-12-2020	DKM2037, DKM2038			

Table 3.1 Performed CPTs, FVTs and boreholes at Westervoort

Date	CPT class 1 (DKM) or CPT class 1 with electric resistivity measurement (DKMG)	CPTu class 2 with $u_2$ measurement	FVT	Borehole
17-9-2019		DKMP1001, DKMP1002, DKMP1003, DKMP1004		
18-9-2019	DKM1005, DKM1006			
25-9-2019				B001
3-10-2019	Start of the monitoring of volumetric water content and suction stress.			
11-10-2019	DKM1007, DKM1008			
23-10-2019			TV101 test 1-6	
24-10-2019	DKM1009, DKM1010		TV101 test 7-10 TV102 test 1	
25-10-2019			TV102 test 2-10	
31-10-2019 / 1-11-2019				B002
14-11-2019	DKM1011, DKM1012			
26-11-2019	DKM1013, DKM1014			
27-11-2019			TV103 test 1-9	
28-11-2019			TV103 test 10-11	
19-12-2019	DKM1015, DKM1016			
13-1-2020	DKM1017, DKM1018			
4-2-2020	DKM1019, DKM1020			
9-3-2020	DKM1021, DKM1022			
8-4-2020	DKM1023, DKM1024			
9-4-2020			TV105	
10-4-2020			TV104	
11-5-2020	DKM1025, DKM1026			
5-6-2020	DKM1027, DKM1028			
29-6-2020	DKM1029, DKM1030			
21-7-2020	DKM1031, DKM1032			
10-8-2020				B003
24-8-2020	DKM1033, DKM1034			
9-9-2020	DKM1035, DKM1036			
10-9-2020			TV107 test 1-12	
11-9-2020			TV107 test 13-18	
14-9-2020			TV106 test 1-11	
15-9-2020			TV106 test 12-18	
30-9-2020	DKMG1047, DKMG1048			
29-10-2020	DKM1037, DKM1038			
3-12-2020	DKM1039, DKM1040			

Table 3.2 Performed CPTs, FVTs and boreholes at Oijen

### 3.2 Volumetric water content measurements

Volumetric water content  $\theta$  is defined as the ratio of the volume of water  $V_w$  to the total volume of the soil  $V$ :  $\theta = \frac{V_w}{V}$ . Gravimetric water content  $w$ , which has been most commonly used in geotechnical engineering, is defined as the ratio of the mass of water  $M_w$  to the mass of soil solids  $M_s$ :  $w = \frac{M_w}{M_s}$ . Volumetric water content is related to gravimetric water content as follows:  $\theta = w \frac{\rho_d}{\rho_w}$ , in which  $\rho_d$  is the dry density of soil and  $\rho_w$  is the density of water.

Water content reflectometers are used to measure the in situ volumetric water content. Measuring water content using a water content reflectometer is an indirect measurement, which is sensitive to the dielectric permittivity of the material surrounding the probe rods. Since water is the only soil constituent that has a high value for dielectric permittivity and is the only component other than air that changes in concentration, a device sensitive to dielectric permittivity can be used to estimate volumetric water content (Campbell, 2016).

The water content reflectometer consists of two stainless steel rods which are connected to an electronic unit with a multivibrator. The applied signal from the multivibrator travels the length of the probe rods and is reflected from the rod ends traveling back to the probe head. When the reflection is detected the next pulse will be triggered. The travel time of the signal from the electronic multivibrator on the probe rods depends on the dielectric permittivity of the material surrounding the rods. The dielectric permittivity depends on the water content. Therefore, the oscillation frequency of the multivibrator depends on the water content of the media being measured. As water content increases, the propagation velocity of the signal decreases because polarization of water molecules takes time. The frequency of pulsing with the probe rods in free air is about 70 MHz. The probe output frequency or period is empirically related to volumetric water content using a calibration equation.

The water content reflectometer operation can be affected when the signal applied to the probe rods is attenuated. The probe will provide a well-behaved response to changing water content, even in attenuating soils, but the response may be different than described by the standard calibration. Consequently, a unique calibration is required. Changes in probe response can occur when soil bulk electrical conductivity is greater than  $0.5 \text{ dS m}^{-1}$ . The major contributor to soil electrical conductivity is the presence of free ions in solution from dissolution of soil salts. Soil organic matter and some clays can also attenuate the signal.

In this project water content reflectometers CS616 of Campbell Scientific are applied. Until now a standard calibration equation for sandy clay loam is applied.

The water content reflectometers are installed in the soil at depths between 1.0 m and 3.25 m below surface level. Details are presented in Table 3.3 and Table 3.4. The devices are installed in boreholes which are drilled with a hand auger. For each device a separate borehole is made. The devices are installed with the probe rods in vertical direction. The probe rods are pushed into the undisturbed soil at the bottom of the boreholes. The boreholes are filled with bentonite after installing the water content reflectometers to prevent for leakage paths around the sensors. Mikolite 00 is used, which has a swelling capacity of 30-40% additional to the bulk volume of the Mikolite when enough water is available.

The measurements of the water content with the four sensors at the outer toe at Westervoort are interrupted from October 1, 2020 to October 15, 2020 due to damage to the cables.



Sensor	Location	Surface level (m + NAP)	Depth of sensor below level (m)	Depth of sensor surface (m + NAP)
1	Outer toe	10.58	0.97	9.61
2	Outer toe	10.59	1.50	9.09
3	Outer toe	10.57	1.85	8.72
4	Outer toe	10.59	3.25	7.34
5	Inner toe	11.26	1.00	10.26
6	Inner toe	11.25	1.50	9.75
7	Inner toe	11.26	2.00	9.26
8	Inner toe	11.27	2.50	8.77
9	Inner berm	10.40	1.00	9.40
10	Inner berm	10.37	1.50	8.87
11	Inner berm	10.41	2.00	8.41
12	Inner berm	10.40	2.50	7.90

Table 3.3 Volumetric water content devices at IJsseldijk Westervoort. The indicated depth of the sensors is halfway the probe rods

Sensor	Location	Surface level (m + NAP)	Depth of sensor below level (m)	Depth of sensor surface (m + NAP)
1	Crest	9.30	1.00	8.30
2	Crest	9.28	1.70	7.58
3	Crest	9.35	2.40	6.95
4	Crest	9.29	3.10	6.19

Table 3.4 Volumetric water content devices at Maasdijk Oijen. The indicated depth of the sensors is halfway the probe rods

### 3.3 Suction stress measurements

To measure the capillary suction (or matric potential) in the field conventional tensiometers are applied. The essential components of conventional tensiometers are a porous filter, a reservoir of liquid (usually water) and a means of measuring stress (Tarantino, Ridley, & Toll, 2008). Tensiometers work by allowing water to move between the water reservoir of the instrument and the soil until the water stress state in both is equal. When water is drawn out of the instrument into the soil tension is caused in the reservoir of liquid. The soil water tension is directly conducted to the pressure transducer which offers a continuous signal.

Conventional tensiometers only cover the range 0-80 kPa, which can be exceeded during the summer period. To date, tensiometers that can measure suction stress continuously over a relatively long period time have a suction range limited to ~80 kPa (Tarantino, Ridley, & Toll, 2008). If the soil dries out the tensiometer runs empty and must be refilled as soon as the soil is sufficiently moist again (Meter, 2018).

In this project the T5 tensiometer of Meter group is used. The measurement range is 100 to -85 kPa, with an accuracy of  $\pm 0.5$  kPa. So, this device can also measure in saturated conditions below the phreatic surface. The T5 tensiometer has a response time of only 5 seconds for a pressure change of 0 to -85 kPa. It reacts very fast to changing soil conditions because of its

small water volume. The atmospheric reference pressure is provided through a membrane on the cable (Meter, 2018).

The tensiometers are installed in the soil at depths between 1.0 m and 3.1 m below surface level. Details are summarized in Table 3.5 and Table 3.6. The devices are installed in separate boreholes which are drilled with a hand auger. The ceramic tip of the tensiometers are pushed into the undisturbed soil at the bottom of the boreholes. After installing the tensiometers the boreholes are filled with bentonite to prevent for leakage paths around the sensors. Mikolit 00 is used, which has a swelling capacity of 30-40% additional to the bulk volume of the Mikolit when enough water is available.

During the dry summer period four tensiometers became outside their measurement range. The porous filters of the sensors then become unsaturated. Therefore, the measurements of these sensors are not reliable anymore. Three of these sensors will be replaced by another type of tensiometer. These tensiometers are ordered and will be installed in the field within a couple of weeks. These are UGT full range tensiometers with a measurement range of -100 (pressure) to 500 kPa or 1500 kPa (suction). The operating principle of the Full Range Tensiometer differs slightly from water filled tensiometers: the measurement volume in the sensor is filled with water that is bonded to a polymer. Due to the bonding of water to the polymer the physical measurement limit of approximately 80 kPa does not account for the Full Range Tensiometer (UGT, 2020). Therefore, the Full Range Tensiometer cannot run dry like conventional water filled tensiometers and is able to measure soil tensions up to 500 or 1500 kPa, respectively.

The measurements of suction with the four tensiometers at the outer toe at Westervoort are interrupted from October 1, 2020 to October 15, 2020 due to damage to the cables.

Sensor	Location	Surface level (m + NAP)	Depth of sensor below level (m)	Depth of sensor (m + NAP)
1	Outer toe	10.60	1.00	9.60
2	Outer toe	10.62	1.50	9.12
3	Outer toe	10.60	2.00	8.60
4	Outer toe	10.60	3.00	7.60
5	Inner toe	11.21	1.00	10.21
6	Inner toe	11.17	1.50	9.67
7	Inner toe	11.19	2.00	9.19
8	Inner toe	11.21	2.40	8.81
9	Inner berm	10.35	1.00	9.35
10	Inner berm	10.36	1.50	8.86
11	Inner berm	10.37	2.00	8.37
12	Inner berm	10.43	2.55	7.88

Table 3.5 Tensiometers at IJsseldijk Westervoort

Sensor	Location	Surface level (m + NAP)	Depth of sensor below level (m)	Depth of sensor (m + NAP)
1	Crest	9.26	1.00	8.26
2	Crest	9.33	1.70	7.63
3	Crest	9.36	2.40	6.96
4	Crest	9.29	3.10	6.19

Table 3.6 Tensiometers at Maasdijk Oijen

### 3.4 Pore water pressure measurements

At the IJsseldijk near Westervoort also piezometers are installed to measure changes in piezometric level in the aquifer and the saturated part of the Holocene clayey cover layer. The piezometer device uses a pressure sensitive diaphragm with a vibrating wire element attached to it (Geokon, 2019). A piezometer incorporates a porous filter stone ahead of the diaphragm, which allows water to pass through but prevents soil particles to act directly on the diaphragm. Standard porous filters are made from sintered stainless steel. Fluid pressures acting at the outer face of the diaphragm cause deflections of the diaphragm and changes in tension and frequency of the vibrating wire. The changes in frequency are sensed and transmitted to the readout device.

In this project Geokon piezometers 4500DP are applied. These piezometers have a pointed nose cone and therefore these devices can be pushed directly into soft ground with drill rods.

Table 3.7 presents the locations and depths of the piezometers at Westervoort.

Sensor	Location	Surface level (m + NAP)	Depth of sensor below surface level (m)	Depth of sensor (m + NAP)
1	Outer toe	10.57	3.62	6.96
2	Outer toe	10.59	4.14	6.45
3	Outer toe	10.61	4.61	6.00
4	Outer toe	10.63	5.62	5.01
5	Outer toe	10.62	6.14	4.48
6	Inner toe	11.08	3.12	7.96
7	Inner toe	11.10	3.64	7.46
8	Inner toe	11.08	4.10	6.98
9	Inner toe	11.08	6.12	4.96
10	Inner toe	11.09	7.13	3.96
11	Inner berm	10.39	3.14	7.25
12	Inner berm	10.39	3.65	6.74
13	Inner berm	10.31	4.12	6.19
14	Inner berm	10.32	4.64	5.69
15	Inner berm	10.32	5.10	5.22

Table 3.7 Pore water measurement devices at IJsseldijk Westervoort

The measurements of piezometric head with the five sensors at the outer toe at Westervoort are interrupted from October 1, 2020 to October 15, 2020 due to damage to the cables.

### 3.5 Cone penetration tests

Cone penetration tests (CPT or CPT<sub>u</sub> when the pore water pressure  $u_2$  is measured) are relatively simple in situ tests. The CPT(u) gives more or less continuous readings of the cone penetration resistance  $q_c$ , sleeve friction  $f_s$  and excess pore water pressure  $u_2$  every 2 cm. The cone penetration test has a relatively small measurement error and high repeatability, depending on the applied accuracy class and the effort in preparation and maintenance of the cone. In the Netherlands CPTs are performed according to NEN-EN-ISO-22476-1. The surface area of the cone is mostly 10 cm<sup>2</sup> and sometimes 15 cm<sup>2</sup>. In this project 10 cm<sup>2</sup> cones are applied. The penetration rate is 2 cm per second. In soft low permeable soils this penetration rate induces undrained soil behaviour. Furthermore, this in situ test is very common in the Netherlands. So, there is a lot of experience with carrying out CPTs and using CPT results in geotechnical analyses.

In this project class 1 cones and class 2 cones are applied. CPT<sub>u</sub>s class 2 are carried out as a preliminary survey. CPTs class 1 are conducted to measure the shear strength of the soil. According to NEN-EN-ISO-22476-1 class 1 CPTs must be conducted including  $u_2$  measurements. As  $u_2$  readings are often unreliable in unsaturated soils the  $u_2$  measurements are not performed. According to NEN-EN-ISO-22476-1 the allowable minimum accuracy of the cone resistance is 35 kPa or 5% for class 1 cones and 100 kPa or 5% for class 2 cones.

Table 3.1 and Table 3.2 give an overview of the CPTs which are performed at Westervoort and Oijen up to now.

#### Derivation of the undrained shear strength

Derivation of the undrained shear strength  $s_u$  from the cone penetration resistance  $q_c$  is not straightforward due to the complex interaction between the soil and the cone. Commonly an empirical relationship between the undrained shear strength and cone penetration resistance is applied:

$$s_u = \frac{q_{net}}{N_{kt}} \quad (3.1)$$

with net cone resistance:

$$q_{net} = q_t - \sigma_{vi} \quad (3.2)$$

and corrected cone resistance:

$$q_t = q_c + u_2(1 - a) \quad (3.3)$$

where:

$N_{kt}$	Empirical correlation factor (-).
$q_t$	Corrected cone resistance for pore pressure effects (MPa).
$\sigma_{vi}$	In situ total vertical stress (MPa).
$\sigma'_{vi}$	In situ effective vertical stress (MPa).
$q_{net}$	Net cone resistance corrected for pore pressure effects and in situ total vertical stress (MPa).
$q_c$	Measured cone tip resistance (MPa).
$u_2$	Pore water pressure measured just behind the cone during penetration (MPa).

$a$  Area ratio (that area affected by the pore water pressure) (-).

Typical values of  $N_{kt}$  are between 10 and 20 (Ladd & DeGroot, 2004; Schnaid, 2009). It is important to note that  $N_{kt}$  depends on the reference strength as the undrained shear strength is not a unique soil parameter but a measure of the strength which depends on several factors. Based on finite element analyses Teh & Houlsby (1988) and Lu et al. (2004) pointed out that  $N_{kt}$  depends on the stiffness of the soil, horizontal stress and roughness of the cone and the shaft.

### Experience in unsaturated soils

Very little is known however on how to interpret the cone penetration test results when performed in unsaturated soils. Equation 3.4 was presented by (Pournaghiazar, Russell, & Khalili, 2013) to correlate changes in cone resistances in unsaturated sand to changes in effective isotropic stress, caused by different suction stress values. The correlation constant  $n$  was derived from a correlation between cone resistance and relative sand density, by assuming that the relative density remains constant for different mean effective stress values.

$$q_{c.2} \approx q_{c.1} \cdot \left( \frac{p'_2}{p'_1} \right)^n \quad (3.4)$$

Where:

- $q_{c.i}$  Cone resistance for different values of the mean isotropic stress (kPa).
- $p'_i$  Mean isotropic effective stress:  $p'$  for different values of the effective suction(kPa).
- $n$  Empirical correlation factor (-).

Regarding cone penetration tests in unsaturated clays, Blight (2013) refers to Powell & Quarterman (1988) who correlated cone penetration data with shear strength back-analysed from plate load test results obtained from various stiff clays and soft rock formations in the United Kingdom. Powell & Quarterman (1988) found a trend of the correlation factor  $N_k$  ( $s_u = \frac{q_c - \sigma_v}{N_k}$ ) to increase with plasticity index (Figure 3.1). In their results was also a distinct influence of the spacing of the cracks and fissures in the clay in relation to the cone size. They distinguished between three classes of spacings: close spacing, intermediate spacing and wide spacing. With wide spacings,  $N_k$  values between 20 and 30 were obtained, whereas  $N_k$  values between 10 and 15 would be appropriate with close spacing.

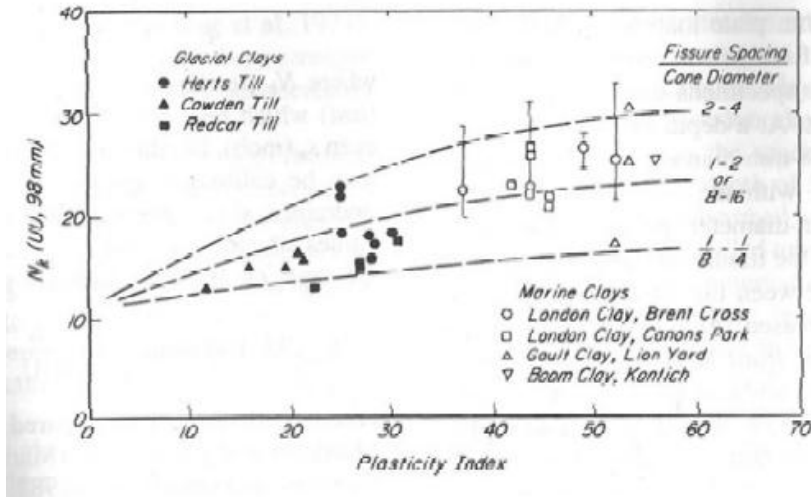


Figure 3.1 The cone resistance in unsaturated aggregated soil is overestimated in case of large distance between the cracks, and the  $N_k$  value should therefore increase (Powell & Quarterman, 1988)

Blight (2013) performed a series of comparative tests at two sites with the cone penetration test and the field vane test. Based on these tests Blight evaluated the correlation factor  $N_k$  for two stiff unsaturated clays in South Africa. Strengths of up to 500 kPa were measured. When relating cone penetration resistance to undisturbed vane shear strength (peak strength) the best average value for  $N_k$  appears to be 15. The data points were in a relatively narrow band.

The in situ measured effect of suction stress on the normalized cone resistance for soils with different plasticity index is shown in Figure 3.2 as reported by Miller et al. (2015). The correlations are weak, however there is a relatively consistent trend of increasing normalized tip resistance with increasing suction stress as expected. An increased value of the normalized cone resistance in combination with increased suction value is only clearly apparent for soils with a large plasticity index. According to Miller et al. (2015) the scatter can be attributed to other factors besides suction that influence the tip resistance, such as variations in soil type, density, degree of weathering, and stress history. The considerable scatter is therefore not surprising since the data represents a variable stratigraphy from zero to about 3 m of depth. Nevertheless, the data provide some insight into potential variations in tip resistance that may occur due to suction changes. Note that the cone resistance has been normalized using the total vertical overburden pressure.

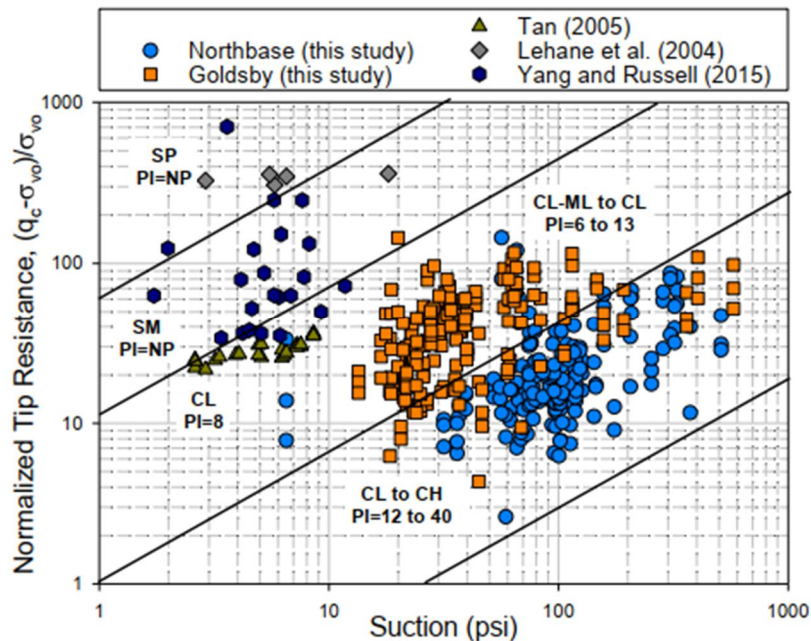


Figure 3.2 Effect of suction on normalized cone resistance, for soils with different plasticity index (Miller, Collins, Muraleetharan, Cerato, & Doumet, 2015). The cone resistance has been normalized using the total vertical overburden pressure

### 3.6 Resistivity Cone Penetration Tests (RCPT)

A CPT device can be equipped with various additional sensors. One of the possibilities is the addition of a module to measure the electrical resistivity (Mayne, 2007; Schnaid, 2009). The resistivity module is located directly behind the friction sleeve. The resistivity module consists of two or more electrodes separated by insulating material. The measurement operates within the principle that the potential drop across two adjacent pairs of electrodes, at a given electrical current, is proportional to the electrical resistivity of both soil and pore fluid. Comparable modules for dielectric measurements are also available. Whereas resistivity induces a direct electrical current into the ground, a similar approach can be provided using alternating current and thus established to obtain dielectric measurements (permittivity).

Measuring the resistivity, conductivity or dielectric constant of the soil during CPT testing would be helpful for the interpretation of CPT results in unsaturated soils. The resistivity, conductivity or dielectric constant are measures of the volumetric water content and via the volumetric water content suction stress can be estimated. In this way using a RCPT could make it possible to estimate suction stress and to interpret the measured cone penetration resistance considering the measured suction stress.

Currently none of the cone manufacturers in the Netherlands can supply a suitable resistivity cone. Some of the cones in the manufacturers delivery programs do not have the appropriate specifications. Other cones cannot be supplied yet because some of the required components are no longer available.

In this project a resistivity cone of Wiertsema & Partners is tested in the laboratory of Deltares and in the field at Westervoort and Oijen. This cone is made by GeoPoint some years ago and is able to measure electrical conductivity (range to 500 mS/m) and dielectric constant (range 1 – 80). The dielectric constant is converted in the CPT-software to the volumetric water content.

### 3.7 Field vane tests

The field vane test (FVT) is applied to determine the in situ peak undrained shear strength and residual shear strength. Table 3.1 and Table 3.2 give an overview of the FVTs which are performed at Westervoort and Oijen up to now.

With a FVT a vane with four rectangular blades is rotated in the soil. It is assumed that a cylindrical shear plane is formed around the rotating vanes. The shear stress on this cylindrical shear plane can be determined based on the torque which is applied to rotate the vane. The failure mode of the FVT is thought to compare with the failure mode of a direct shear test (Chandler, 1988).

FVTs are usually applied to determine the in situ undrained shear strength of saturated soft soils. The undrained shear strength is calculated from the torque which is required to rotate the cylinder of soil within the four vane blades. When rotating the vane first the undisturbed or peak strength is measured and after five to ten rotations the remoulded vane shear strength is measured. Standards for FVT are ASTM D 2573-01 and FprEN 22476-9:2010.3.

There is a lot of experience with the application of these tests in saturated conditions. Empirical corrections based on plasticity index (Bjerrum, 1972; Chandler, 1988) or liquid limit (Larsson, Bergdahl & Eriksson, 1987) are used to derive the undrained shear strength from the measured torque. The empirical corrections are applied to account for the complex failure mode and rate of strain of the FVT. The corrections are based on back-analyses of failures of embankments and footings. So, these empirical corrections assure that the measured torque reflects the operational undrained shear strength of the investigated soft soils.

Drainage conditions of the FVT are a point of particular interest. To determine the in situ undrained shear strength the drainage conditions during performance of a FVT have to be fully undrained. In permeable soils this will not be the case when applying the standard rotation rate.

Blight (2013) mentions the FVT to determine the shear strength of unsaturated soils. This author presents some cases where the FVT is applied in residual weathered sandstone and mudstone and residual shales. The author states that the remoulded strength of the FVT approximates to the strength of the soil en masse in stiff jointed or fissured soils. Issues related to the empirical corrections which are based on the experience with saturated soft soils are not mentioned by this author.

#### Interpretation

For standard vane dimensions with the height of the vane two times the diameter of the vane the undrained shear strength  $s_{u,FVT}$  of the soil can be determined with FprEN 22476-9:2010.3:

$$s_{u,FVT} = 0.273 \frac{T}{D^3} \quad (3.5)$$

Where:

$T$  torque on the vane (kNm).  
 $D$  diameter of the vane (m).

To convert the FVT measurements to an accurate estimation of the operational shear strength there are several issues to be considered, such as friction along the rods, shear stress distribution on the vane blades, anisotropy of the soil, rate effects, and partial consolidation



(Chandler, 1988; Schnaid, 2009). The friction along the rods plays no role in this project as a FVT device is applied with the motor just above the vane.

### **Stress distribution and anisotropy**

The shear stress distribution on the vane blades is uncertain. Several studies are conducted to determine the stress distribution on the vane blades. Anisotropy of the undrained shear strength due to the soil fabric developed during deposition and consolidation effects enhance the complexity of the shear stress distribution on the vane. When considering stress distribution and anisotropy a number of variations on equation 3.5 are possible (Schnaid, 2009). Equation 3.5 as proposed by FprEN 22476-9:2010.3 assumes isotropic soil conditions and uniform stress distribution on the vanes. Applying other assumptions, the calculated undrained shear strength may deviate substantially, at least when anisotropy is large. Bjerrum (1973) showed that the anisotropy of the undrained shear strength is low for soils with plasticity index above 40%. Assuming isotropic soil conditions and uniform stress distribution yields a low estimate of the undrained shear strength. As the stress distribution and anisotropy are very difficult to assess in practice equation 3.5 as proposed by FprEN 22476-9:2010.3 is commonly adopted (Schnaid, 2009). The resulting undrained shear strength is then corrected with empirical corrections which account for several aspects, such as strain rate, soil disturbance and anisotropy of the shear strength.

Becker et al. (1988) proposed that the FVT interpretation could be refined when the in situ horizontal effective stress and horizontal yield stress would be considered. As the common practice uses the vertical effective stress and empirical correlations are also based on the vertical effective stress in the present research also the vertical effective stress will be used. For CPT interpretation the horizontal stress also plays a role (see Paragraph 0), but for CPT interpretation also the vertical stress is commonly applied.

### **Rate effects**

Rate effects are important because the rotation of the vane is much faster than the rate of a slope failure. As the undrained shear strength exhibit rate dependency, correction for rate effects is required. This correction is generally incorporated in empirical corrections for the FVT. The empirical corrections are derived using a rotation rate of 6 degrees/minute. This rotation rate is also applied in this project.

### **Empirical corrections**

Bjerrum (1972) derived an empirical correction factor  $\mu$  to adjust the measured undrained shear strength from the FVT to the operational undrained shear strength in the field. This correction factor is related to the plasticity index  $I_p$  and accounts for effects of shear strength anisotropy and strain rate. Bjerrum obtained the correction factor from back calculated case histories. The correction factor decreases from 1.1 for  $I_p$  is 10% to 0.55 for  $I_p$  is 120%. The correction factor is applied as follows:

$$S_{u,field} = \mu S_{u,FVT} \quad (3.6)$$

Azzouz et al. (1983) also examined the required correction of the measured undrained shear strength from the FVT. These authors pointed out that Bjerrum (1972) ignored three-dimensional effects in the back-analyses of the case histories. Therefore, the correction factor proposed by Bjerrum can be reduced by some 10% for field conditions with a plane strain mode of failure (see Figure 3.3).

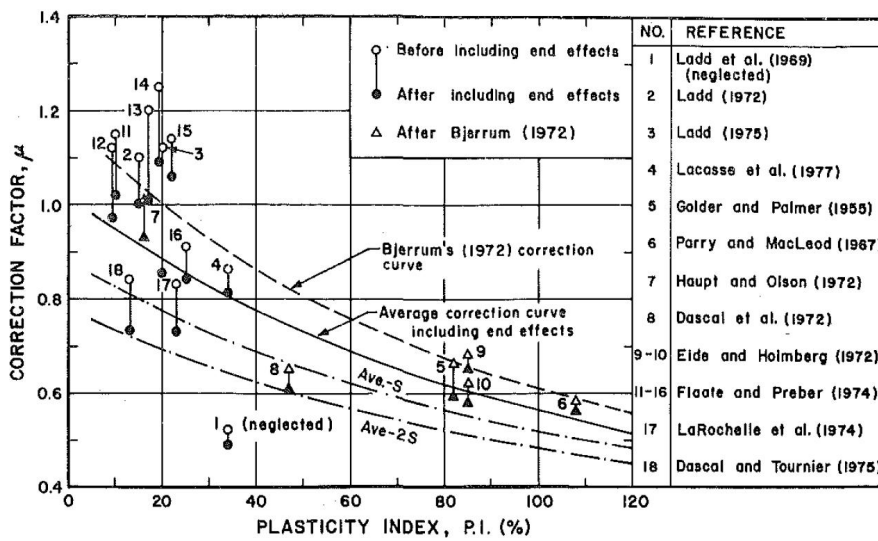


Figure 3.3 Correction factor to adjust FVT measurements (Azzouz et al., 1983). The correction factor is based on back-analyses of failures. Be aware of the considerable uncertainty of the correction factor

A widely used correction for the FVT measurements is suggested by Chandler (1988). This correction is also based on the plasticity index. The Chandler correction depends on the time to failure for the construction for which the correction factor is required (not the time to failure in the FVT). The Chandler (1988) correction corresponds with the correction of Azzouz et al. (1983) for the time to failure of  $10^4$  minutes. The Chandler correction is:

$$\mu_R = 1.05 - b (I_p)^{1/2} \quad \text{with } b = 0.015 + 0.0075 \log t_f \quad (3.7)$$

Where:

$I_p$  Plasticity index (%).  
 $t_f$  Time to failure (min).

In Swedish practice the empirical correction for FVT as proposed by Larsson et al. (1987) and Larsson et al. (2005) is used. Instead of the plasticity index the liquid limit  $w_L$  is applied. The Larsson correction is largely based on high plastic soils, whereas the Bjerrum correction is mainly based on low- and medium plastic clays (Larsson et al., 1987). The lower limit of the Larsson correction is 0.5, which is based on Swedish experience with qualified laboratory investigations on organic soils with very high plasticity. For soils with overconsolidation ratio  $OCR$  larger than 1.3 an additional correction is applied. The FVT correction from Larsson et al. is the product of  $\mu$  and  $\mu_{OCR}$  as follows:

$$\mu = \left( \frac{0.43}{w_L} \right)^{0.45} \geq 0.5 \quad \text{and} \quad \mu_{OCR} = \left( \frac{OCR}{1.3} \right)^{-0.15} \quad (3.8)$$

where:

$w_L$  liquid limit (%).

### 3.8 Boreholes

Mechanical drillings using the Ackermann sampling system are carried out in accordance with NEN-EN-ISO 22475-1 and BRL SIKB 2100, protocol 2101. The boreholes are carried out as a pulse bore system. Inside the casing samples have been taken each 0.5 m from surface level. The Ackermann sampling tubes are 0.4 m long. The sampling tubes have a diameter of 67 mm. The sampling tubes are pushed into the soil.

Table 3.1 and Table 3.2 give an overview of the boreholes which are performed at Westervoort and Oijen up to now.

### 3.9 Classification tests

The following classification tests are carried out in the laboratory:

- Determination of the bulk volume weight is carried out in accordance with NEN-EN-ISO 17892-2, Geotechnical investigation and testing - Laboratory testing of soil - Part 2: Determination of bulk density. The bulk volume weight of the complete samples from the sampling tubes is determined. The linear measurement method according to the aforementioned ISO standard is used.
- Determination of the gravimetric water content is carried out by drying samples in the oven according to NEN-EN-ISO 17892-1, Geotechnical investigation and testing - Laboratory testing of soil - Part 1: Determination of water content.
- Determination of the Atterberg limits is carried out according to NEN-EN-ISO 17892-12, Geotechnical investigation and testing - Laboratory testing of soil - Part 12: Determination of Atterberg limits. Only test samples consisting of fine soil (primary fraction of clay or silt) are tested. The determination of liquid limit is carried out with the fall cone; 4-point method.
- Determination of the grain size distribution is carried out in accordance with NEN-EN-ISO 17892-4, Geotechnical investigation and testing - Laboratory testing of soil - Part 4: Determination of particle size distribution. Only test samples consisting of fine soil (primary fraction of clay or silt) are tested using sieves from 0.002 mm to 2.0 mm.
- Determination of the specific gravity of the solid is carried out in accordance with NEN-EN-ISO 17892-3, Geotechnical investigation and testing - Laboratory testing of soil - Part 3: Determination of particle density. Only test samples consisting of fine soil (primary fraction of clay or silt) are tested. The liquid pycnometer method is used.
- Determination of the organic matter content is carried out according to NEN-EN-ISO 14688-2, Geotechnical investigation and testing - Identification and classification of soil - Part 2: Principles for a classification. Only test samples consisting of fine soil (primary fraction of clay or silt) are tested. The determination is carried out with hydrogen peroxide as described under NB.2 of NEN-EN-ISO 14688-2 starting from clay as the main soil type.
- Determination of specific surface using a surface area analyser with nitrogen gas (N<sub>2</sub>) as an adsorbate. The Brunauer, Emmett, and Teller (BET) gas adsorption theory (Brunauer et al, 1938) is applied to determine the volume of gas required to form a unimolecular layer of gas on adsorbents and to compute specific surface. Determination of the specific surface area is not covered in the ASTM and NEN-EN-ISO standards. The specific surface can be determined by various instruments and methodologies. To perform the N<sub>2</sub> BET tests the descriptions in Santamarina et al. (2002), Arnepalli et al. (2008) and Akin et al. (2014) are followed.

So far classification tests are conducted on samples of borehole B001 from Oijen and B201 from Westervoort. For each sample (0.4 m) these classification tests are carried out by Wiertsema & Partners, resulting in profiles with depth of the concerning soil properties.

Determination of specific surface is performed on samples of borehole B003 from Oijen and B203 from Westervoort by Delft Solids Solutions.

### 3.10 Determination of shear strength in the laboratory

In order to interpret the shear strength measurements in the field (CPTs and FVTs) different tests to measure shear strength are performed in the laboratory. These tests are conducted on intact samples and on reconstituted samples. Laboratory tests on intact samples are meant to investigate the relationship between water content, suction and shear strength and to verify the measured shear strength in the field. For this goal unconsolidated undrained (UU) triaxial compression tests, direct shear tests and direct simple shear tests are conducted.

The aim of the tests on reconstituted samples is to investigate the causes of the relatively high shear strength which is found by the CPTs and FVTs in the field during winter period when suction is negligible (see Paragraph 4.5). Reconstituted samples are tested with isotropic consolidated undrained (CIU) triaxial compression tests. Reconstituted samples are prepared from a slurry and from moist material. The slurry is made applying a water content corresponding to 1.25 times the liquid limit  $w_L$ . The slurry samples are dried in the air to simulate the effect of ripening of clay, which occurs in nature after sedimentation of clayey material due to interaction with the atmosphere. The slurry samples are dried to different target water contents. After drying the samples are saturated, consolidated and sheared in a triaxial apparatus to simulate saturated conditions like winter conditions in the field. Moist samples are compacted with a Proctor mould and a Proctor hammer according to ASTM D 698 with applying a different number of blows and different water content to get different samples with a range of densities. These moist compacted samples are intended to investigate the effect of compaction on shear strength of dike material when building a dike. After compaction the samples are saturated, consolidated and sheared in a triaxial apparatus to test the samples at saturated conditions like winter conditions in the field.

The reconstituted samples are based on material from borehole B203 from Westervoort, samples 1, 3 and 5, and borehole B003 from Oijen, samples 1, 4, 6, 7, 9 and 10.

#### Triaxial tests

Unconsolidated undrained (UU) triaxial compression tests and isotropic consolidated undrained (CIU) triaxial compression tests are conducted according to NEN-ISO 17892-8 and NEN-ISO 17892-9 respectively. The protocol (Deltares, 2016) is also applied.

UU triaxial tests are performed on intact samples with 67 mm diameter. To test the samples in their intact state the samples are not saturated and not consolidated. With the used triaxial apparatus suction in the samples cannot be measured. Therefore, the influence of suction on measured shear strength with these UU tests have to be interpreted by applying the relationship between water content and suction (retention curve; see Paragraph 3.12). The samples are sheared to 25% axial strain.

CIU triaxial tests are conducted on reconstituted samples. These samples are prepared in the laboratory and are saturated and consolidated in a triaxial apparatus as mentioned above. For the moist compacted tests 67 mm samples are applied. For the tests on the slurry samples 50 mm diameter samples are used to save time with drying and consolidation of the samples.

### **Direct simple shear tests**

Direct simple shear tests are performed according to ASTM D 6528-07 and the Deltares protocol (2016). Direct simple shear tests are performed with constant vertical load, to be able to determine the dilatancy angle.

The samples are tested in their intact state, without saturation and consolidation. Similar to the UU triaxial tests the results of the direct simple shear tests have to be interpreted by using the relationship between water content and suction from the retention curves. The samples are sheared to 40% shear strain.

The intact samples are prepared carefully to place them on the end plates with pins. Because some of the intact samples were very stiff, they could not be prepared to place the sample on the end plates with the pins or the ridges. Therefore, direct shear tests are performed for the very stiff intact samples.

### **Direct shear tests**

Direct shear tests are conducted according to ASTM D 3080. Direct shear tests are performed with constant vertical load, in order to determine the dilatancy angle. Direct shear tests are executed on very stiff samples which could not be tested in the direct simple shear apparatus. Furthermore, the test procedure of the direct shear test is similar to the procedure of the direct simple shear test.

### **Oedometer tests**

Oedometer tests are performed according to NEN-EN-ISO 17892-5 and the Deltares protocol (2016). Oedometer tests are conducted on intact samples and reconstituted samples (slurry). The results of these tests are helpful for the interpretation of the soil behaviour and for the interpretation of the results of the shear strength tests.

The laboratory tests to investigate the relationship between water content, suction and shear strength are performed by the geotechnical laboratory of TU Delft. The other laboratory tests are executed by the geotechnical laboratory of Deltares.

## **3.11 Proctor test**

A standard Proctor test is conducted to get insight in the relationship between water content and dry unit weight. The dry unit weight is a measure of the density of the sample which can be achieved given the amount of water in the sample. Water content in the sample has a relationship with suction when the samples become unsaturated and a relationship with shear strength.

The standard Proctor test is performed according to the Dutch code RAW 2015 test 9.0. The Proctor tests are carried out on a mixed sample based on borehole B001 from Oijen, samples 21 - 27 (6,7 kg), and borehole B201 from Westervoort, samples 15 - 19 (5,3 kg). According to the classification tests as reported in Paragraph 4.8 these samples have comparable soil properties. A series of triaxial tests is conducted on reconstituted samples, which are derived from a mixed sample, which is composed in the same way from samples of boreholes B003 and B203. The Proctor test is performed by the laboratory of Wiertsema & Partners.

## **3.12 Determination of retention curves and shrinkage curves**

For unsaturated soils the relationship between water content and suction, the soil water retention curve, is relevant to understand soil behaviour. The retention properties of a series of

samples have been investigated with the Hyprop device (Meter Group). The HYPROP consists of a main sensor unit comprising two tensiometers of different lengths. An 80 mm stainless steel ring with a 50 mm height is used for containing the soil sample that is placed on the sensor unit. The entire setup sits on top of a weighing scale to measure the increase or decrease of water content. The air-entry value of the ceramic tips is 880 kPa, but as the water in shaft cavitates earlier, the maximum suction that can be measured is approximately 100 kPa.

The HYPROP data allows inferring the response of the soil (e.g. with a van Genuchten's model) for both drying and wetting events, which will facilitate the interpretation of the shear strength data, beyond their dependence on the water content.

The HYPROP tests are performed by the geotechnical laboratory of TU Delft.

As the volume of a soil sample changes during drying or wetting the degree of saturation also changes. This behaviour is measured in shrinkage tests. In a shrinkage test the relationship between water content and void ratio is measured. These shrinkage tests are performed by the geotechnical laboratory of TU Delft.

### 3.13 Mercury intrusion porosimetry tests

The pore size distribution (PSD) of 12 samples is determined using mercury intrusion porosimetry (MIP). This technique gives a useful quantitative characterization of microstructure of a soil sample. In the MIP test a sample is immersed in mercury and a pressure is applied to the mercury such that the mercury enters the pores. To perform a MIP test the water that occupies the pores has to be removed because the water will prevent the entry of mercury. Drying the samples is performed with the freeze-drying technique. With the MIP test the entrance diameters of the pores can be detected as the entrance pore diameter, contact angle between mercury and the pore walls and the surface tension of mercury determines the required mercury pressure.

The MIP test is described in ISO 15901-1:2016 and ASTM D 4404-18. The procedures to prepare the samples with freeze drying technique and to perform the MIP tests is derived from Mitchell et al. (2005), Romero et al. (2008), Koliji et al. (2010) and Liu et al. (2015). The MIP tests are performed by Delft Solids Solutions.

Integration on PSD data of the pore volume between the minimum detectable pore size and the delimiting pore size, normalised by solid volume gives the microstructural void ratio. The delimiting pore size is the pore size at the boundary of the PSD function between the region where the macro pores are dominant and where the micro pores are dominant. These void ratios of the macro pores and the micro pores will be used to determine the effective degree of saturation as only the capillary suction in the macro pores contribute to the shear strength.

## 4 Results

### 4.1 Introduction

In this chapter the results of the monitoring of volumetric water content, suction stress and pore water pressure at the measurement locations Westervoort and Oijen are presented. The results of the in-situ measurements of the shear strength, as determined with the cone penetration tests and field vane tests, are also presented in this chapter. Six boreholes are conducted until now. The in-situ descriptions of these boreholes are presented in Appendix A for the location Westervoort and Appendix B for the location Oijen. On samples of these boreholes classification tests and various laboratory tests are performed. The results of these tests are summarized in this chapter.

### 4.2 Volumetric water content measurements

Volumetric water content is measured at the locations Westervoort and Oijen. The type of the applied sensors and the locations of the sensors are described in Paragraph 3.2.

Hitherto a standard calibration equation from the manufacturer of the sensors is used. This means that the presented values of volumetric water content are not necessarily correct. The calibration equation will be adjusted by a customized calibration equation based on laboratory test results later in the project.

Figure 4.1 – Figure 4.4 present the measured volumetric water content at Westervoort and Oijen. The values between brackets in the legends are the positions of the sensors below surface level. The measurements of the water content with the four sensors at the outer toe at Westervoort are interrupted from October 1, 2020 to October 15, 2020 due to damage to the cables.

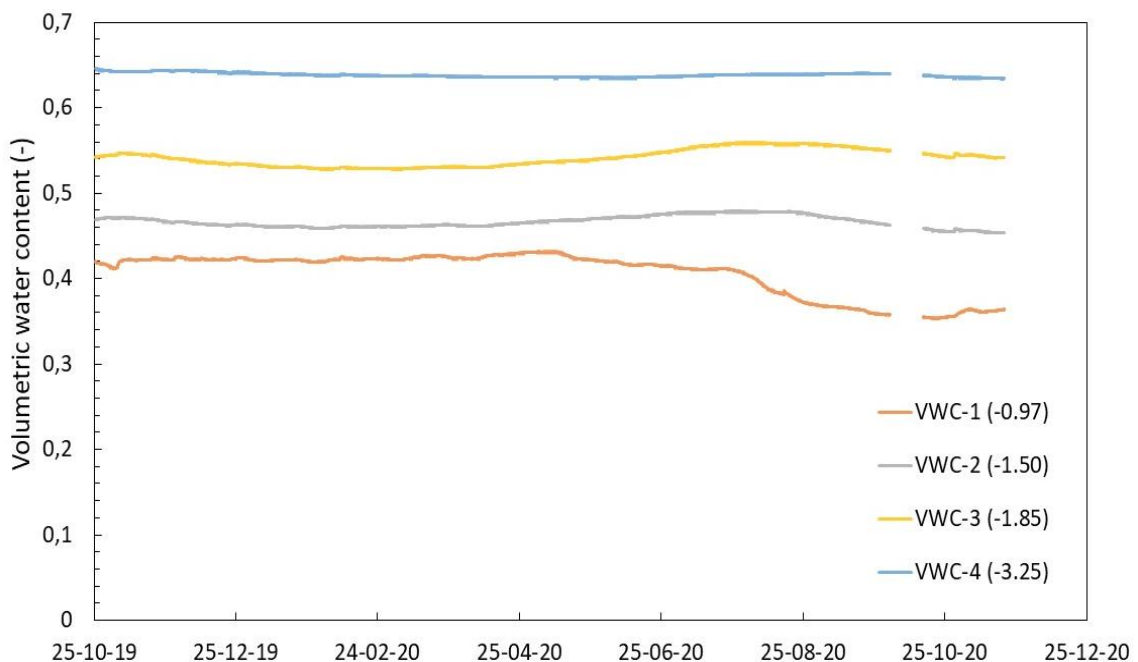


Figure 4.1 Measured volumetric water content at Westervoort at the outer toe

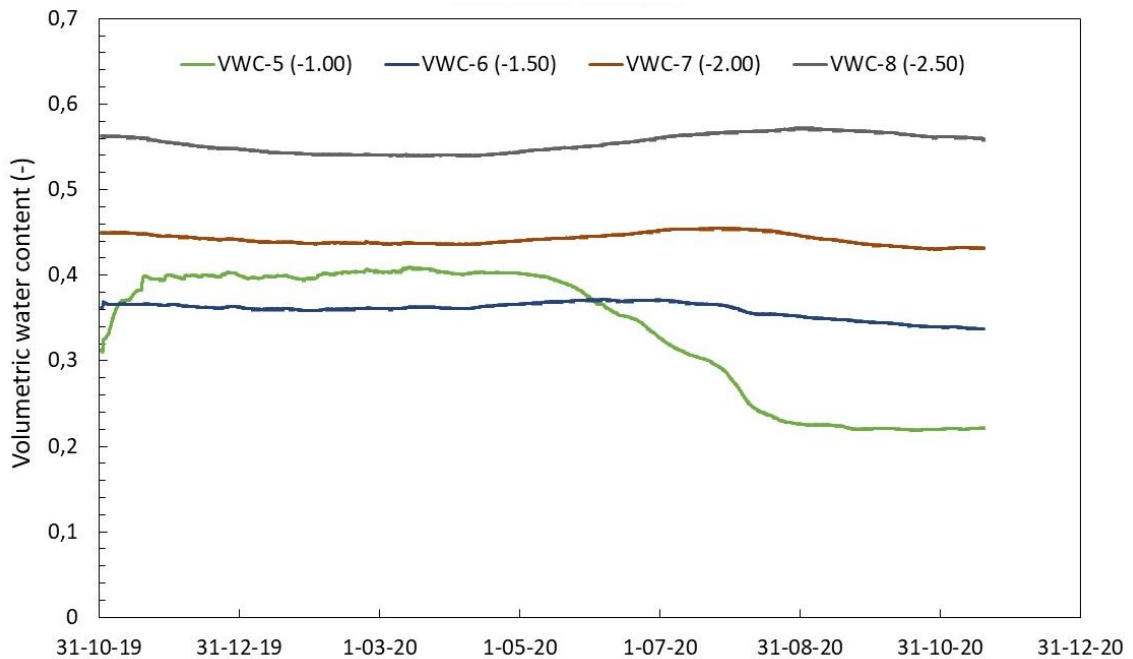


Figure 4.2 Measured volumetric water content at Westervoort at the inner toe

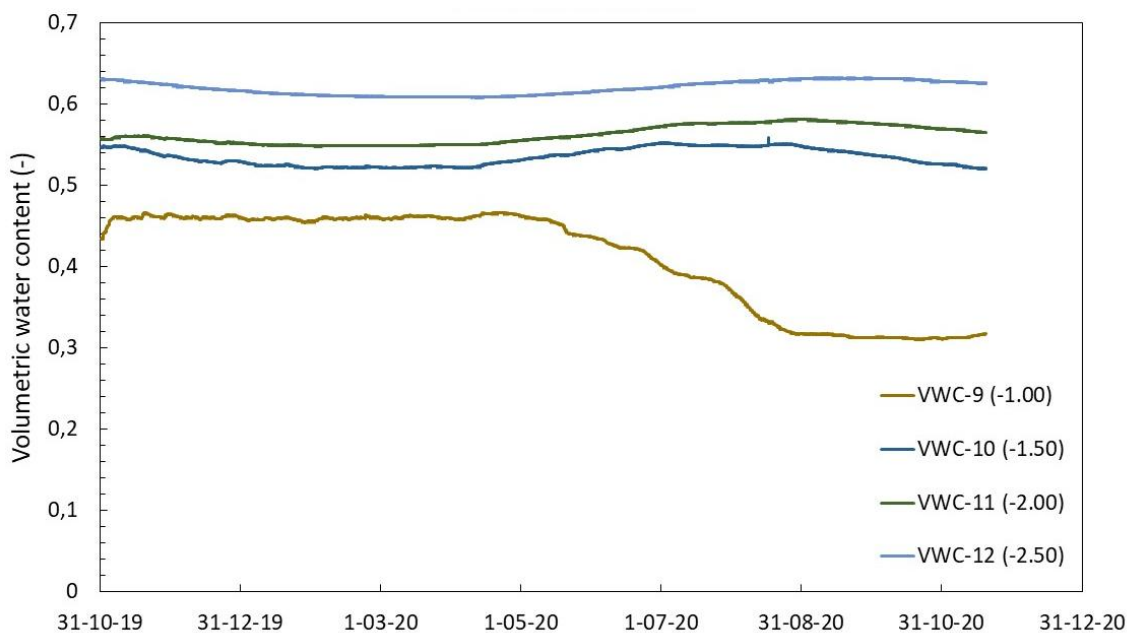


Figure 4.3 Measured volumetric water content at Westervoort at the inner berm

VWC-1, VWC-5 and VWC-9, which are the shallowest sensors, show the largest fluctuations of water content. During summer water content decreases and reaches the minimum values at the end of the summer and beginning of the autumn, which will reflect the interaction with the atmosphere. The results of the volumetric water content measurements of the deeper sensors at Westervoort show overall a relatively constant volumetric water content. Interestingly the deeper sensors show the maximum water content when the shallow sensors have their minimum values. For each of the three locations, the volumetric water content increases in depth. An exception is found at the inner toe, Figure 4.2 for which the shallowest transducer,



VWC-5 indicates a larger volumetric water content than the second largest transducer VWC-6 during October 2019 to July 2020. VWC-5 and VWC-9, which are installed at 1.0 m depth, show an increase of the volumetric water content in the first weeks after installation. This effect can be attributed to installation effects or probably to precipitation.

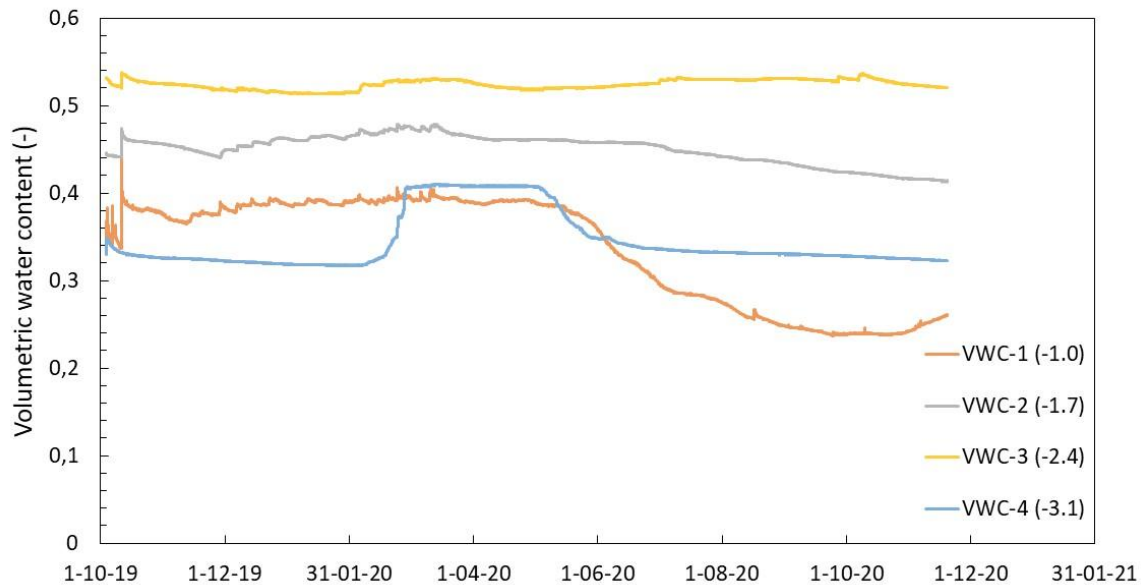


Figure 4.4 Measured volumetric water content at Oijen

The sensors VWC-1, VWC-2 and VWC-3 at Oijen in Figure 4.4 show some fluctuations in the first two weeks after installation of the sensors. These fluctuations can at least partly be attributed to installation effects, due to adding water to the bentonite by which the boreholes are filled after installation of the sensors. At October 11 again water is added to the bentonite in the boreholes. The sensors respond to that action. It seems that the measurement results are reliable from the end of October. The shallow sensor VWC-1 shows the same behaviour as the shallow sensors at Westervoort, with decreasing water content during summer and reaching the minimum values at the end of the summer and beginning of the autumn. VWC-1 and VWC-2, which are the shallowest sensors, also show fluctuations from November and December and beyond. From February similar fluctuations are present for the deeper sensor VWC-3. In this period the sensors show an increasing trend. Likely these fluctuations are induced by precipitation. During the second part of the winter and in spring VWC-4 measured a clearly higher water content compared to the rest of the year.

### 4.3 Suction stress measurements

As described in Paragraph 3.3 suction stress is measured at the measurement sites Westervoort and Oijen. The type of the applied sensors and the locations of the sensors are described in Paragraph 3.3. Figure 4.5 – Figure 4.8 present the measured suction stress at Westervoort and Oijen. The values between brackets in the legends are the positions of the sensors below surface level. The measurements of suction with the four tensiometers at the outer toe at Westervoort are interrupted from October 1, 2020 to October 15, 2020 due to damage to the cables. During the dry summer period four tensiometers became outside their measurement range. The porous filters of the sensors then become unsaturated. Therefore, the measurements of these sensors are not reliable anymore and are therefore not presented.

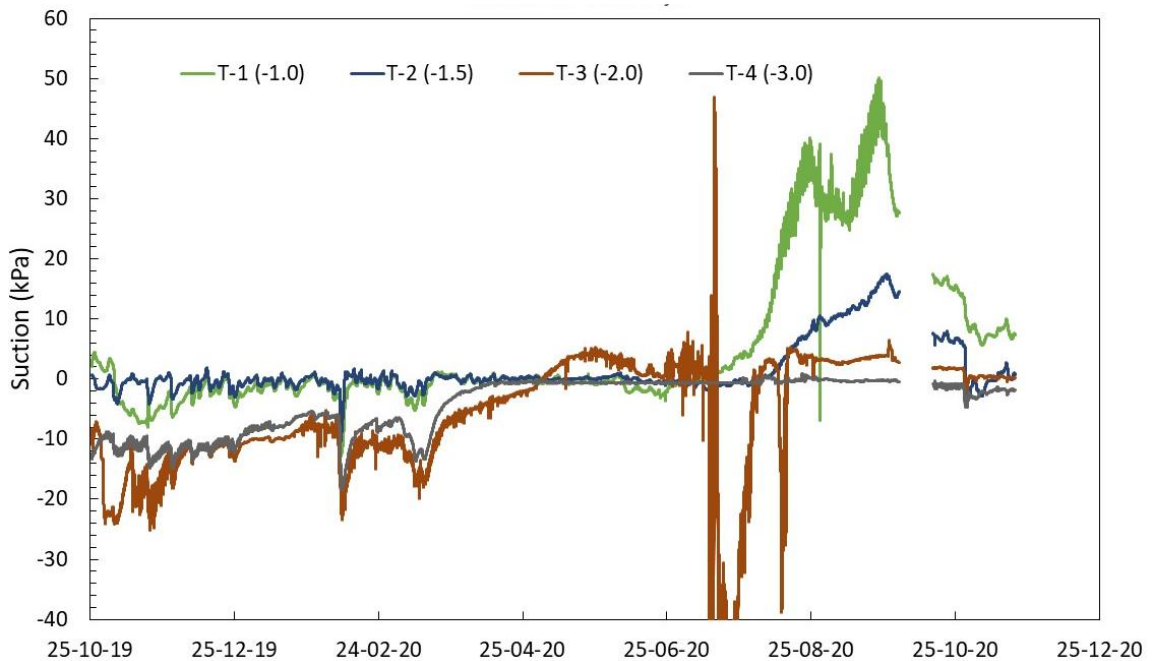


Figure 4.5 Measured suction stress at Westervoort at the outer toe

The sensors T-3 and T-4 at Westervoort in Figure 4.5 show some noise. The noise disappeared temporarily in December for sensor T-3 and in January for sensor T-4 but returned at the end of January for sensor T-3. It is not clear yet what the reason for this noise is. It is believed that at least the noise of sensor T-3 is too large to be related with a physical phenomenon in the soil. These two sensors will be replaced by other devices.

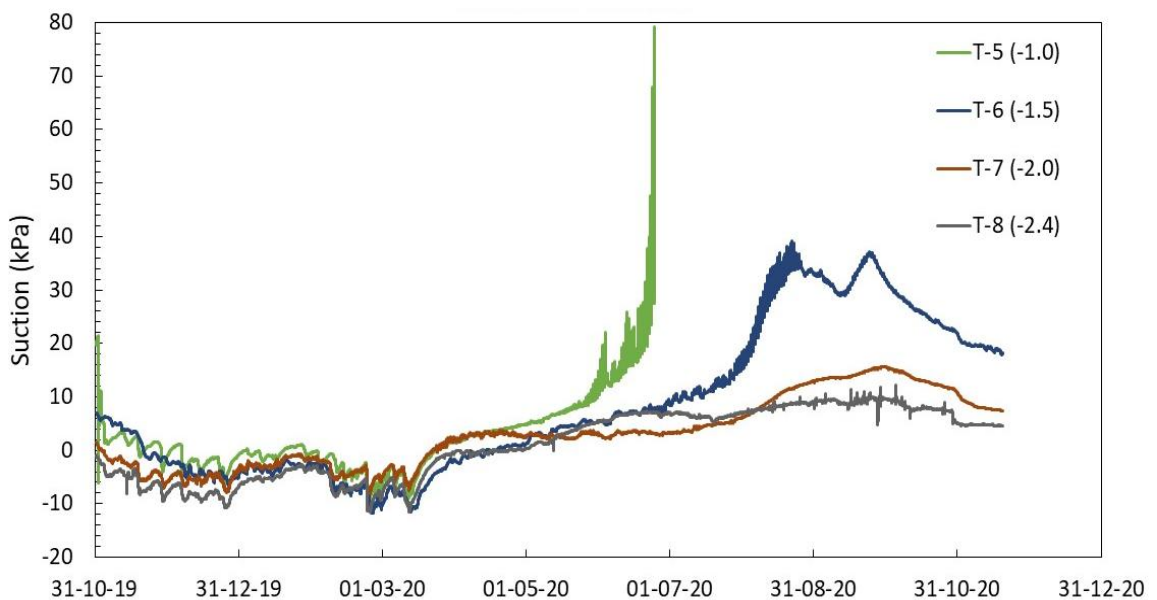


Figure 4.6 Measured suction stress at Westervoort at the inner toe

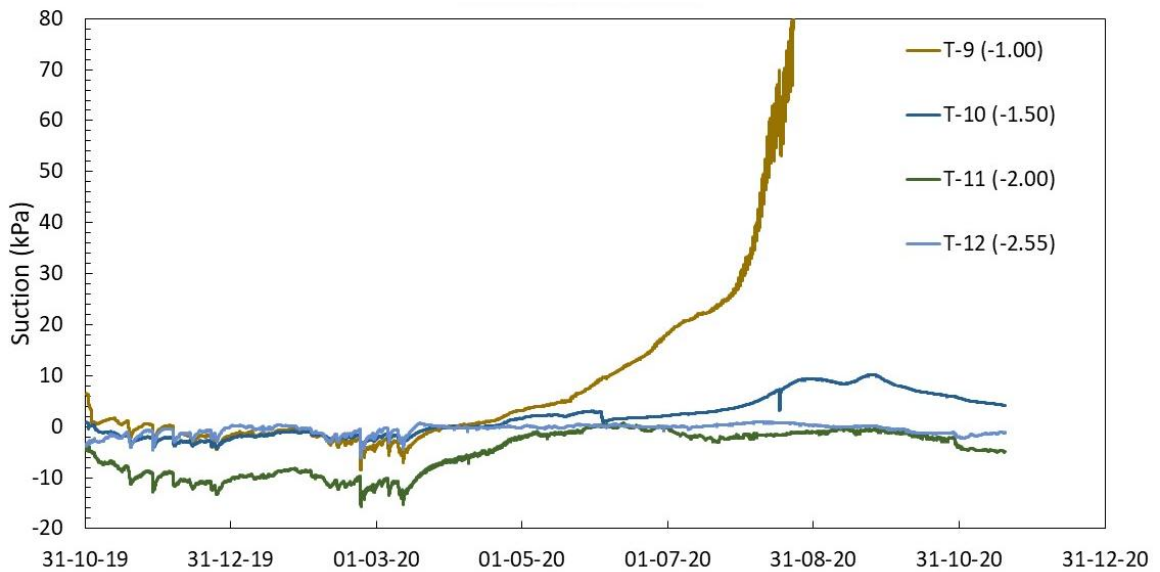


Figure 4.7 Measured suction stress at Westervoort at the inner berm

For all sensors at Westervoort suction has become negative in winter period in Figure 4.5 - Figure 4.7, implying positive pore water pressures. So, the level of the phreatic surface is in winter period above the sensors. During summer period the shallowest sensors reach suction values from 30 kPa and beyond 80 kPa. The sensors at 1.5 m depth reach suction values between 10 and 40 kPa.

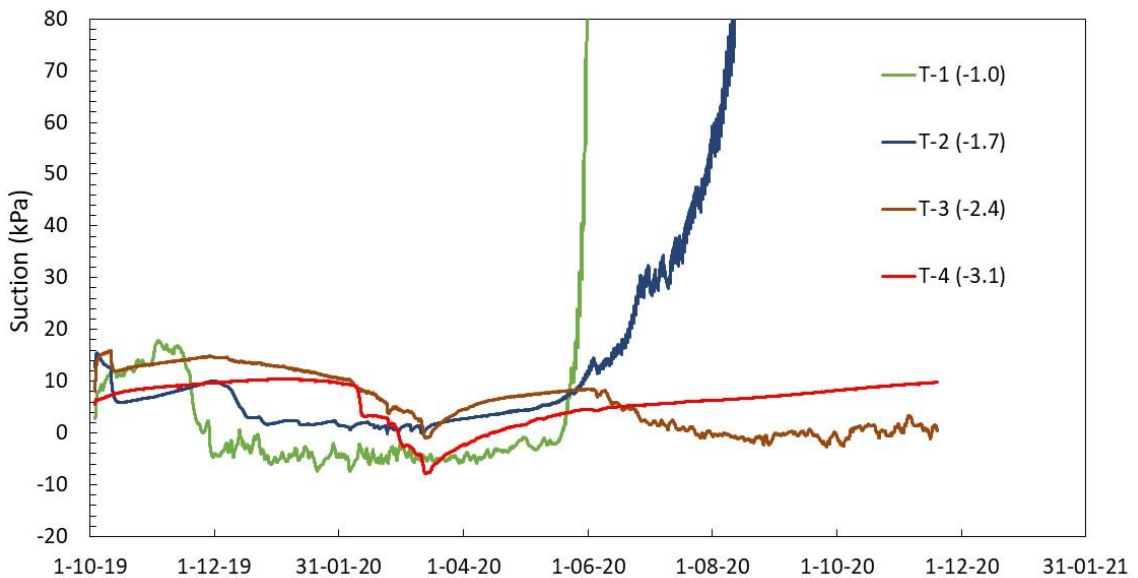


Figure 4.8 Measured suction stress at Oijen

The sensors T-2 and T-3 at Oijen in Figure 4.8 show firm fluctuations in the first two weeks after installation of the sensors. After installation of the sensors the boreholes are filled with bentonite and water is added to the bentonite. At October 11 again water is added to the bentonite in the boreholes. The sensors respond to these actions. During October 2019 the sensors T-2, T-3 and T-4 show a continuous increase of suction stress. In this period the sensors move towards an equilibrium with the surrounding soil. It seems that the measurement

results of the sensors T-2, T-3 and T-4 are reliable from the end of November 2019, as the increase of the previous period has stopped, and the sensors seem to respond to precipitation. Sensor T-1 show a rapid drop to negative suction in the last part of November and in December. This means that fully saturation and positive water pressure is reached. This implies a phreatic surface in de top of the dyke. In December 2019 and January and February 2020 the suction of the other sensors also declined to lower values, but these values are still positive (suction 1-4 kPa). For sensors T-2 and T-4 this declination of suction also occurred rapidly. Only a few days in March all sensors show negative suction values (pressure) and thereafter suction starts to increase again. The shallow sensor T-1 shows a very rapid increase of suction in the end of May and exceeds the measurement range. Sensor T-2 exceeds the measurement range in August. Suction in the other two sensors stays below 10 kPa.

#### 4.4 Pore water pressure measurements

Pore water pressure is measured at the measurement site at Westervoort, as described in Paragraph 3.4. The type of the applied sensors and the locations of the sensors are described in Paragraph 3.4. Figure 4.9 – Figure 4.11 show the measured piezometric head at Westervoort. The values between brackets in the legends are the positions of the sensors relative to reference level NAP. The measurements of piezometric head with the five sensors at the outer toe at Westervoort are interrupted from October 1, 2020 to October 15, 2020 due to damage to the cables.

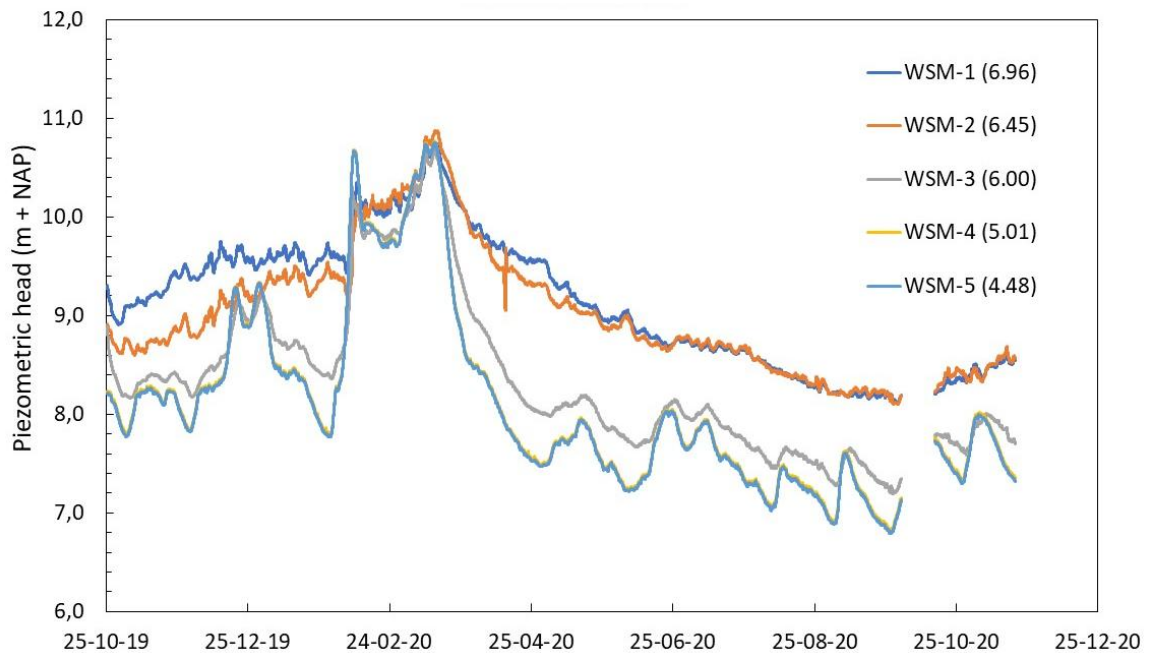


Figure 4.9 Measured piezometric head at Westervoort at the outer toe

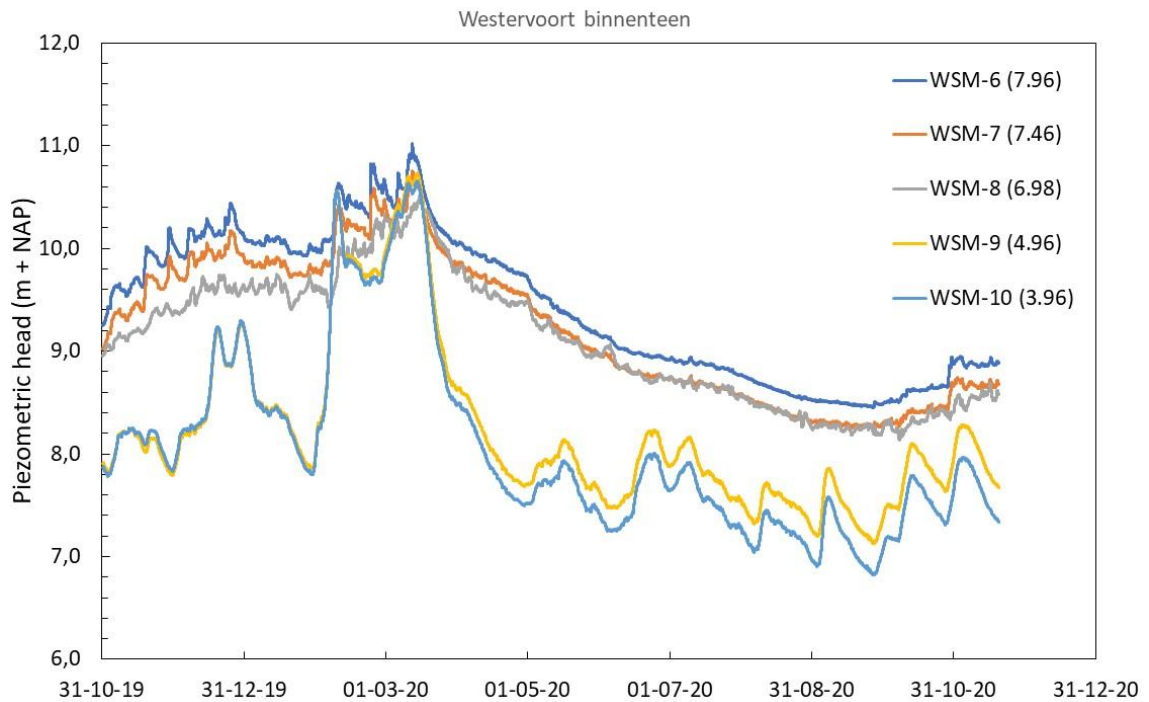


Figure 4.10 Measured piezometric head at Westervoort at the inner toe

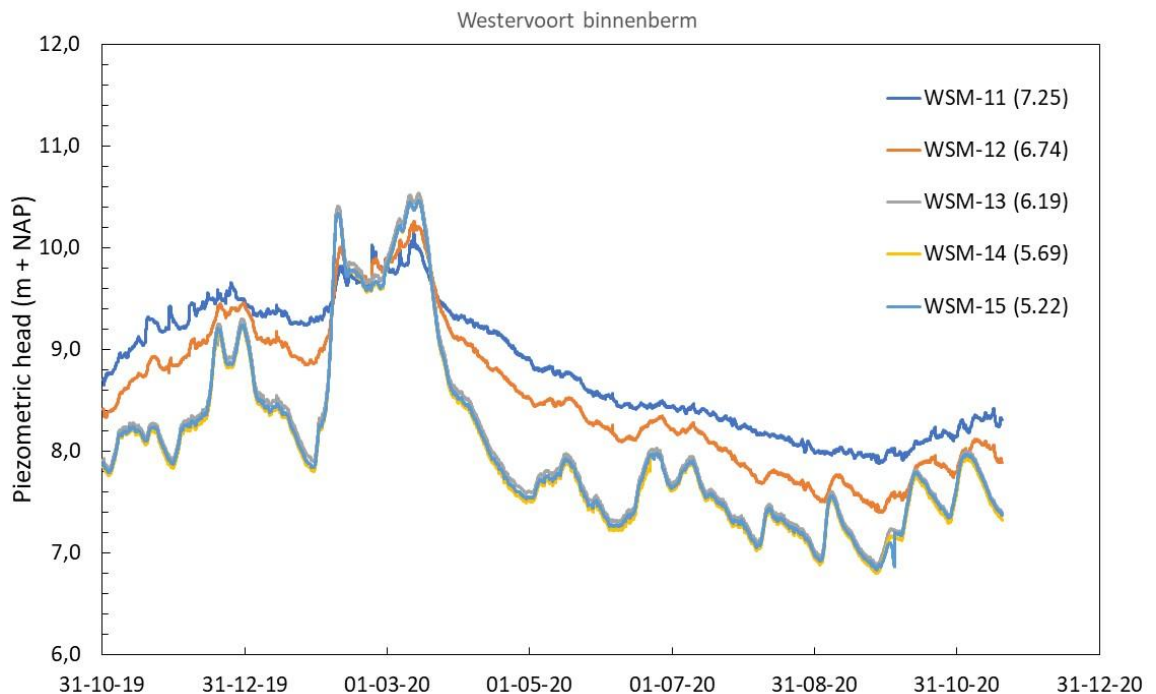


Figure 4.11 Measured piezometric head at Westervoort at the inner berm

The piezometric heads decline from the highest piezometers to the deepest piezometers at normal circumstances. This is the case at the outer toe, inner toe and inner berm. So, the piezometric head is higher in the clayey cover layer compared to the sand layer (aquifer). The difference in piezometric head between the clay layer and sand layer is up to 2.0 m. The difference in piezometric head in vertical direction between two piezometers can be up to 0.8

m over 0.5 m. At high-water conditions in February and March groundwater flow is in the reversed direction, with a relatively rapid response of the pore water pressure in the clayey cover layer.

#### 4.5 Cone penetration tests, field vane tests

Cone penetration tests (CPT) and field vane tests (FVT) are conducted to measure the in-situ shear strength. Backgrounds of these tests can be found in Chapter 3. As described in Paragraph 3.1 CPTs class 2 are performed for a first investigation of the sites. CPTs class 1 are executed to measure the in-situ shear strength.

Figure 4.12, Figure 4.13 and Figure 4.14 present the results of the FVT and CPT (class 1) of the location Westervoort. The FVT correction using the Chandler (1988) correction is applied with plasticity index  $I_p$  as presented in Paragraph 4.8 and using a time to failure  $t_f$  of 360 min. The shear strength is derived from the CPTs using ( $s_u = \frac{q_c - \sigma_v}{N_k}$ ). The pore water pressure  $u_2$  is not incorporated in this analysis, as  $u_2$  is not measured with the class 1 CPTs, because the reliability of the  $u_2$  measurements in the unsaturated zone is questionable. For the CPT interpretation a soil unit weight of 18.0 kN/m<sup>3</sup> is assumed. A  $N_k$  value of 11.0 is used to fit the CPT data to the FVT results. For each FVT this single  $N_k$  value agrees well with the CPTs.

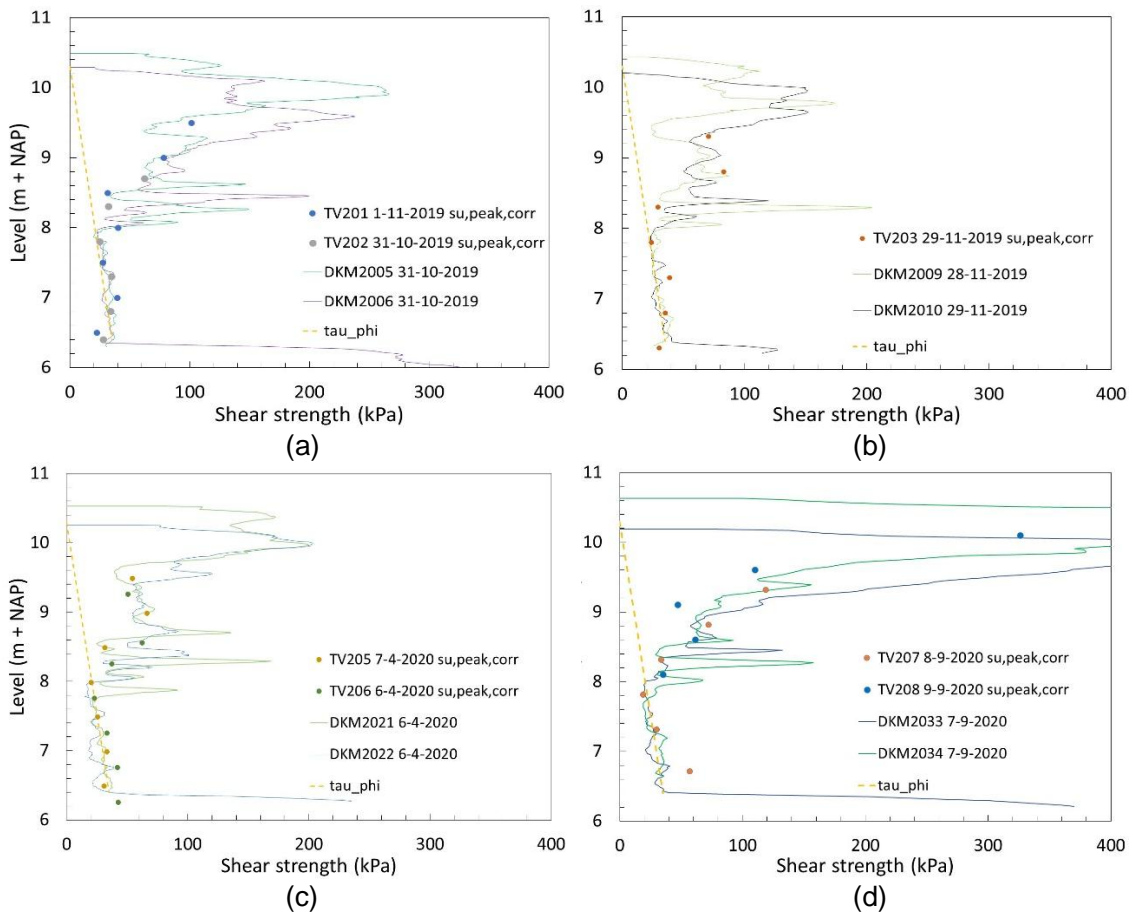


Figure 4.12 FVT and CPT (class 1) results of location Westervoort at four times during the measurement period

Using the  $N_k$  value of 11.0 Figure 4.13 and Figure 4.14 show the derived shear strength from the CPTs. Because of the large number of CPTs to be presented and because of the fact that

the CPTs are conducted in double each time the even numbers of the CPTs are presented in Figure 4.13 and the odd numbers are presented in Figure 4.14 .

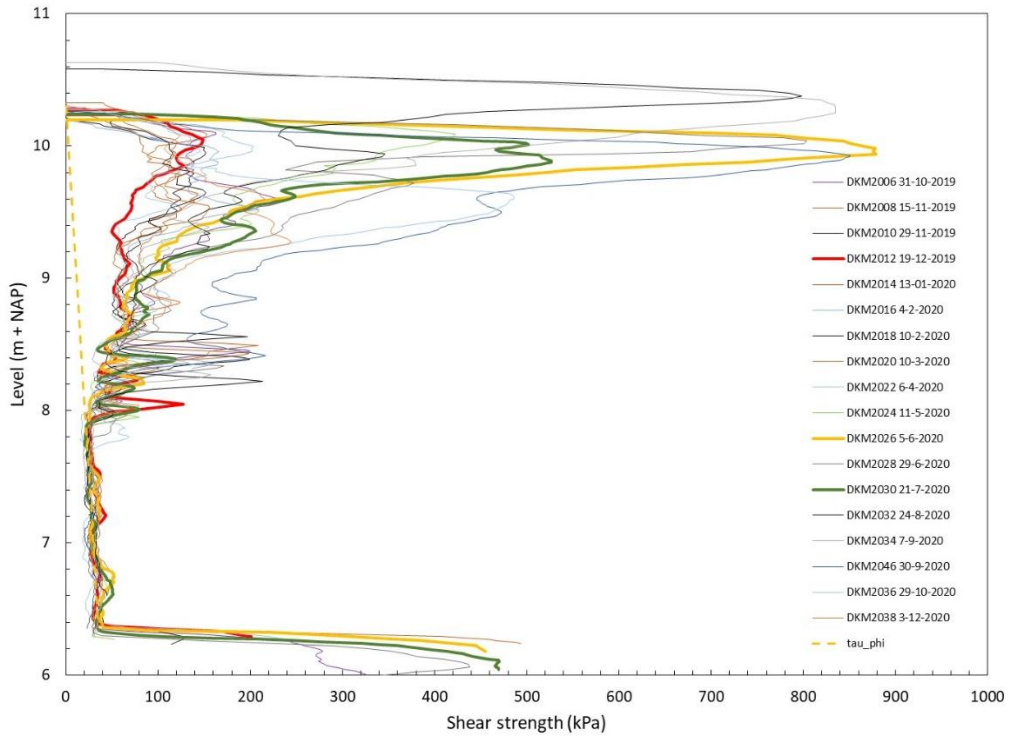


Figure 4.13 CPT (class 1, even numbers) results of location Westervoort

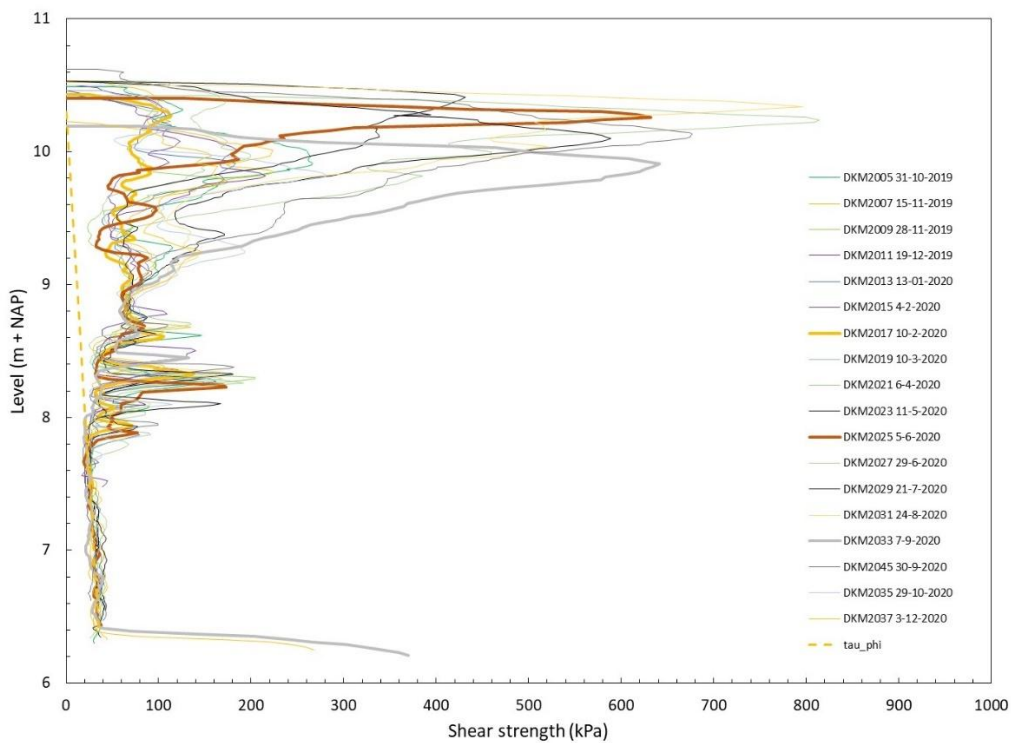


Figure 4.14 CPT (class 1, odd numbers) results of location Westervoort

The transition between the stable pattern of the shear strength profile below NAP +8.0 m and the scatter of the shear strength above NAP +8.0 m at Westervoort in Figure 4.13 and Figure 4.14 coincide with the average lowest phreatic level (GLG in Dutch) as determined from the borehole B201 (see Appendix A). The shear strength above NAP +8.5 m generally varies with time, but the natural variability of the shear strength gives much scatter. To highlight the effect of the seasonal variation of the shear strength some of the CPTs are plotted with bold lines. Figure 4.13 and Figure 4.14 generally give the same pattern. It can be seen that shear strength is relatively low in the second part of the winter. In spring shear strength increases. High shear strength values are measured at shallow depth. In summer the shear strength also increases at larger depth, but due to precipitation the shear strength near surface level can be lower compared to spring. Note that the shear strength as derived from FVTs and CPTs is substantially larger than the drained shear strength based on friction angle (yellow dashed line, assuming a friction angle of 30°) even when suction is reduced to very low values during February and March 2020 as discussed in Paragraph 4.3.

The results of the FVT and CPT (class 1) of the location Oijen are presented in Figure 4.15, Figure 4.17 and Figure 4.17. The FVT results are corrected again using the Chandler (1988) correction (see Paragraph 3.7) with  $I_p$  as presented in Paragraph 4.8 and using a time to failure  $t_f$  of 360 min. The tests are performed each 0.5 m in the dyke and Holocene clay layers. A  $N_k$  value of 17.0 is applied to fit the CPT data to the FVT results. Here again this single  $N_k$  value gives a good agreement for each FVT with the accompanying CPTs. The relationship between FVT and CPT results seems to be not sensitive for the effect of suction in the top layers.

Using the  $N_k$  value of 17.0 Figure 4.16 and Figure 4.17 show the derived shear strength from the CPTs. In Figure 4.16 the odd numbers of the CPTs are presented and in Figure 4.17 the even numbers are presented.



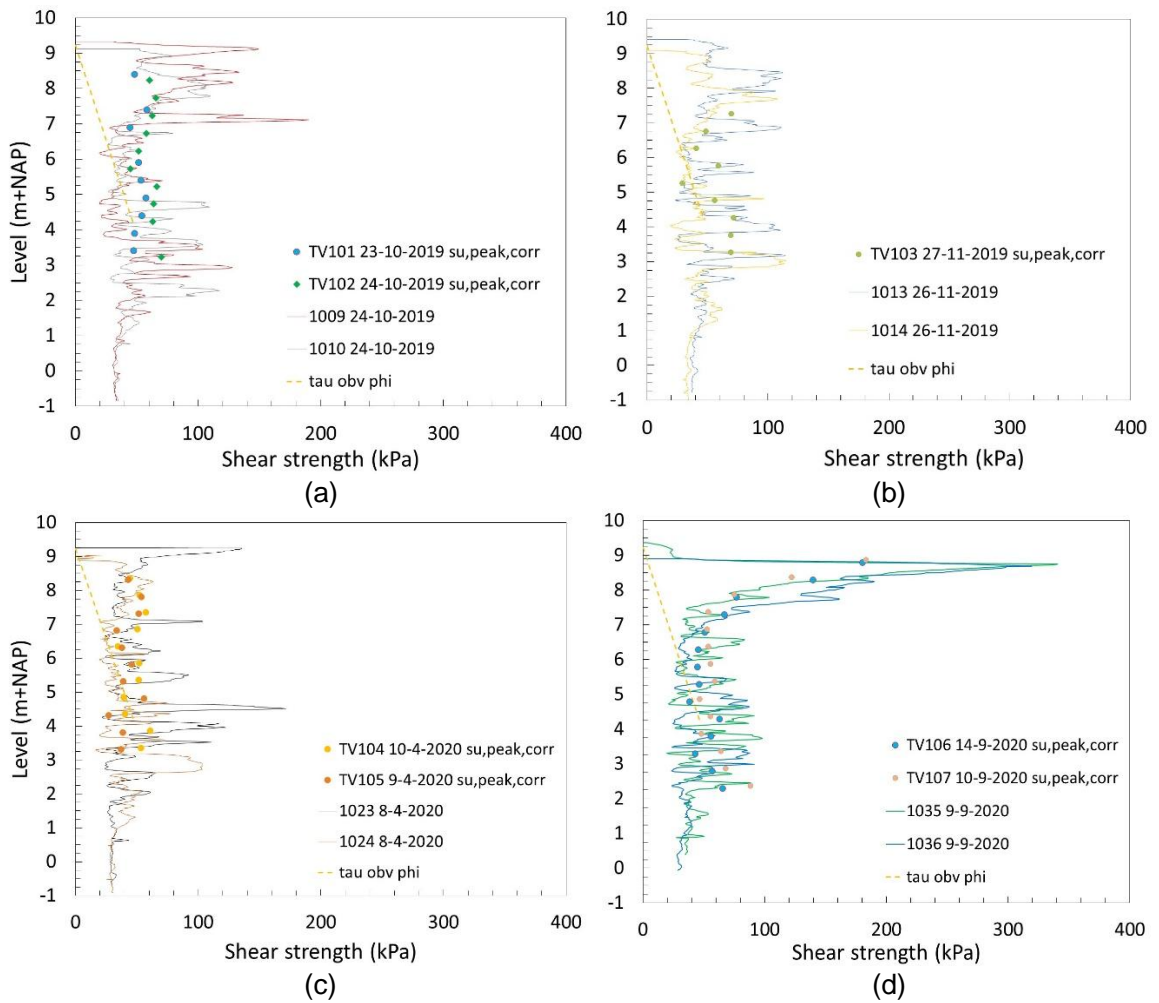


Figure 4.15 FVT and CPT (class 1) results of location Oijen

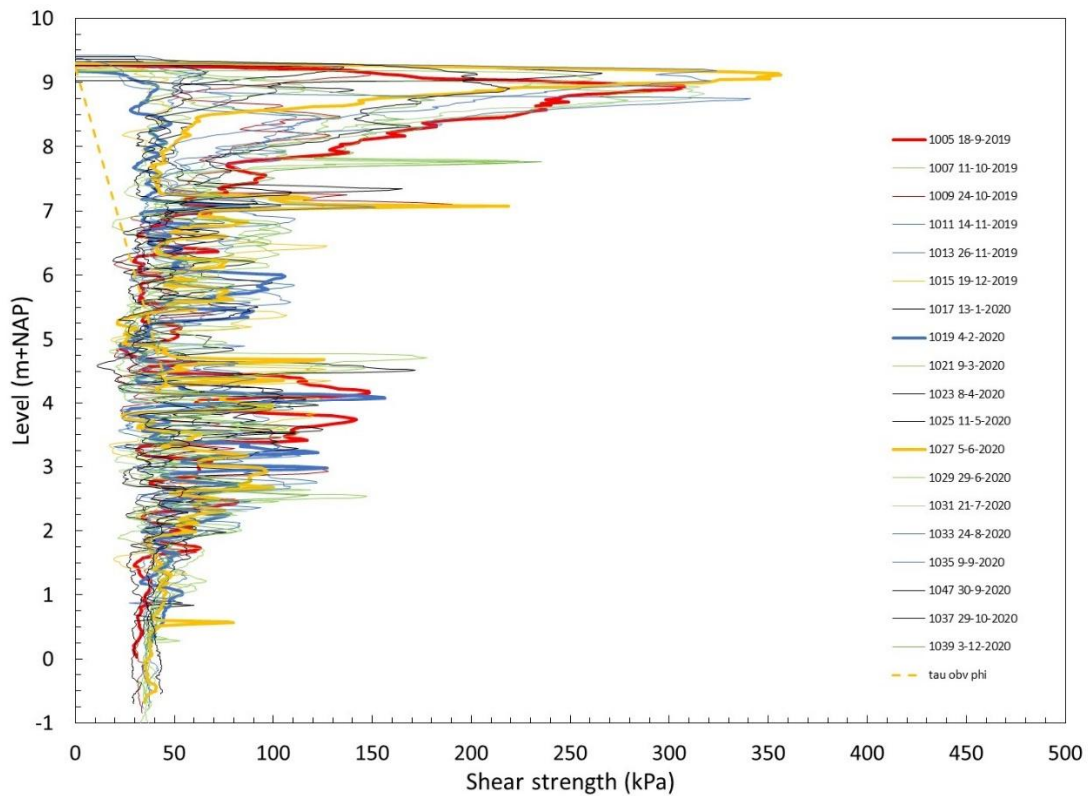


Figure 4.16 CPT (class 1 odd numbers) results of location Oijen

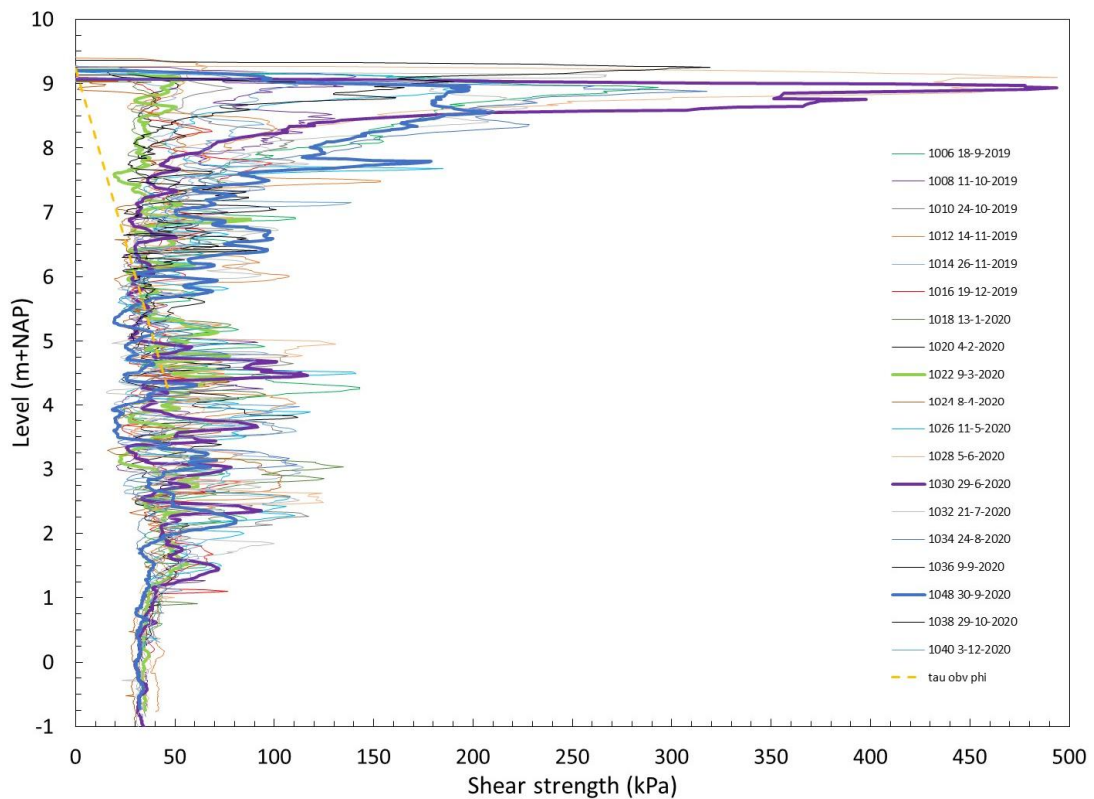


Figure 4.17 CPT (class 1 even numbers) results of location Oijen

The shear strength derived from the cone penetration resistance at Oijen shows the same seasonal pattern as the shear strength at Westervoort. In Figure 4.16 and Figure 4.17 this is highlighted with the bold lines. At Oijen the influence of the interaction of the subsoil with the atmosphere reaches a depth of about 4.0 m. Similar to the results at Westervoort the shear strength as derived from FVTs and CPTs is substantially higher than the drained shear strength based on friction angle (yellow dashed line in Figure 4.16 and Figure 4.17, assuming a friction angle of 30°). Natural variability of the shear strength is also remarkably at Oijen. Note that the first two CPTs at Oijen are carried out in mid-September, but the monitoring of water content and suction stress at Oijen started at the beginning of October. Therefore, the high cone resistances of the first two CPTs in September cannot be correlated to measurements of suction stress and water content.

#### 4.6 Resistivity Cone Penetration Tests (RCPT)

In this project a GeoPoint resistivity cone of Wiertsema & Partners is tested in the laboratory of Deltares and in the field at Westervoort and Oijen. To get a first idea about the validity of the electrical conductivity and volumetric water content measurements some simple tests are performed in the laboratory:

- Tests to verify the volume which is measured by the cone in horizontal and vertical direction.
- Measurements in dry sand and water with increasing salt content.
- Measurements in sand with various water contents.
- Measurements in clay samples with decreasing water content.

Some of the most important findings from these tests are:

- There seem to be an offset of 10% water content.
- The measured water content in sand seem to be plausible.
- For clays the measured water content can deviate from the real water content. Therefore, calibration is required based on the soil to be tested.
- The measured temperature by the cone seems to be incorrect. The electrical conductivity depends on temperature.

The results of the tests in the laboratory are reported in Deltares (2019d). The findings as summarized above are discussed with Wiertsema & Partners and GeoPoint. After that the resistivity cone is tested at Oijen and Westervoort to compare the measurements with the results of the volumetric water content sensors.

The results of the tests in the field are presented in Figure 4.18. At each site two RCPTs with measurement of the electrical conductivity are performed to get insight in the variability of the electrical conductivity. The RCPTs are performed at September 30, 2020. The results of the electrical conductivity measurements are compared with the volumetric water content measurements from the sensors at the timespan when the RCPTs are conducted. To get a good comparison between the electrical conductivity from the CPTs with the volumetric water content from the sensors the electrical conductivity had to be divided by 130. Note that this factor will be dependent on the soil type (clay content and organic content), water content and temperature. So, proper calibration is always required, however Figure 4.18 illustrates that the RCPT has the potential to be a useful tool to determine the water content and to be able to determine the influence of suction on the cone penetration resistance, as the water content can be used to estimate suction.

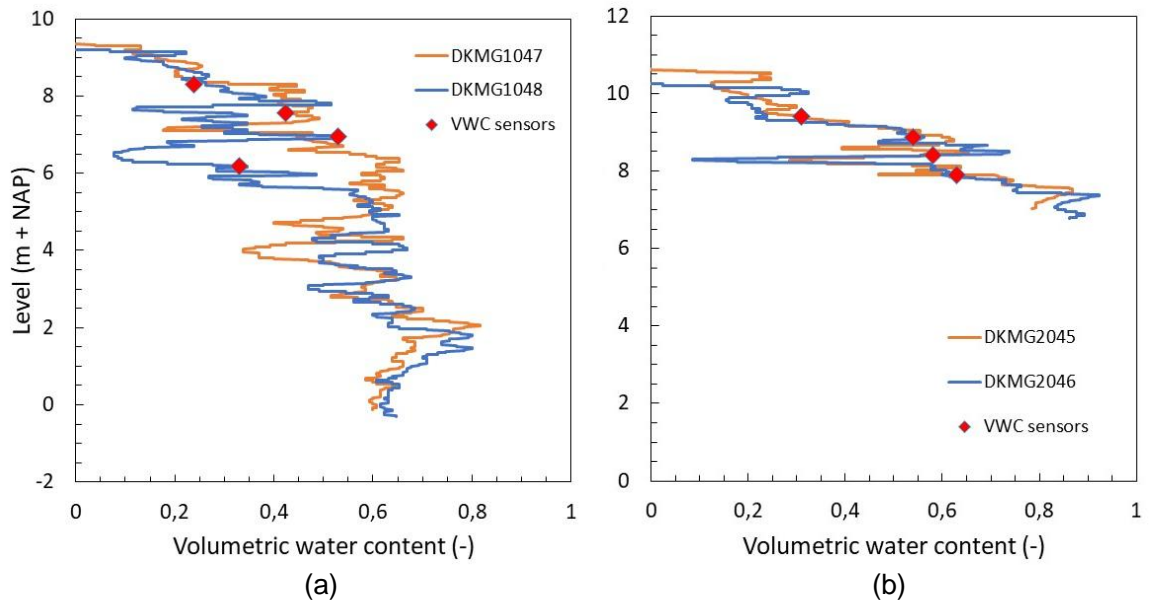


Figure 4.18 Comparison of the results of the electrical conductivity measurements from the RCPT and volumetric water content measurements from the sensors at Oijen (a) and Westervoort (b). A factor 130 is used for both sites to get a good comparison

#### 4.7 Boreholes

The descriptions of the boreholes are presented in Appendix A for the location Westervoort and Appendix B for the location Oijen.

#### 4.8 Classification tests

The results of the classification tests as performed on the samples from borehole B201 at Westervoort are summarized in Figure 4.19 - Figure 4.21.

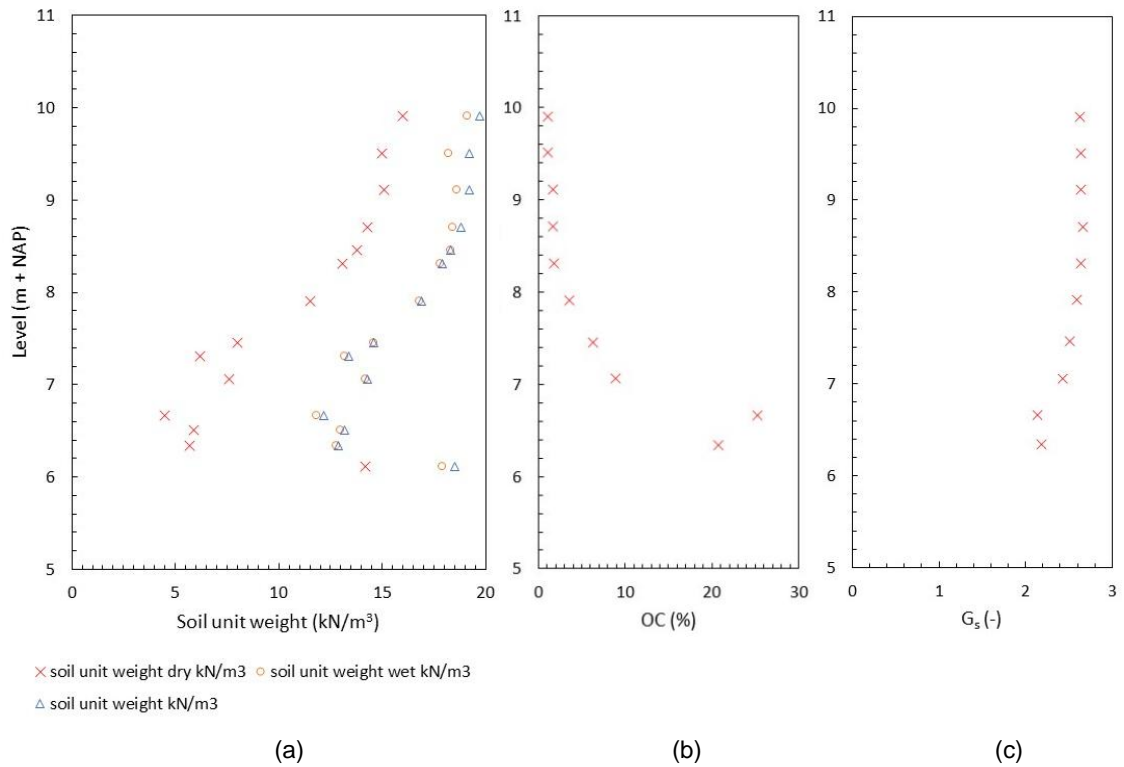


Figure 4.19 Profiles of (a) soil unit weight, (b) organic content (OC) and (c) specific gravity of the soil particles ( $G_s$ ) against depth from borehole B201 at Westervoort

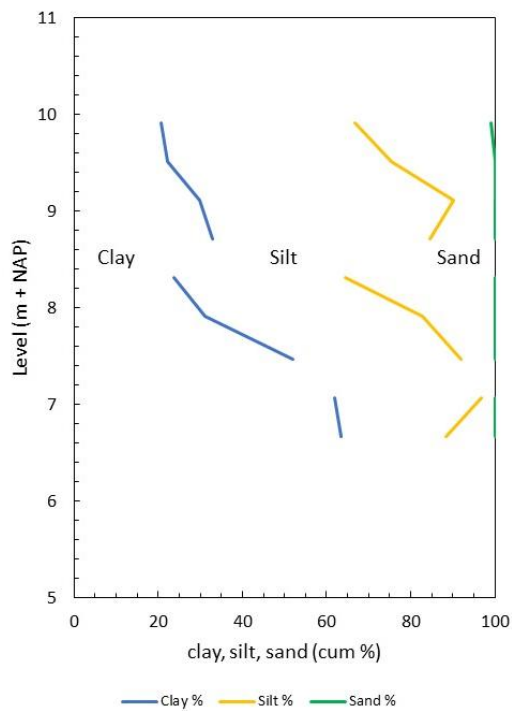


Figure 4.20 Profile of clay, silt and sand content against depth from borehole B201 at Westervoort

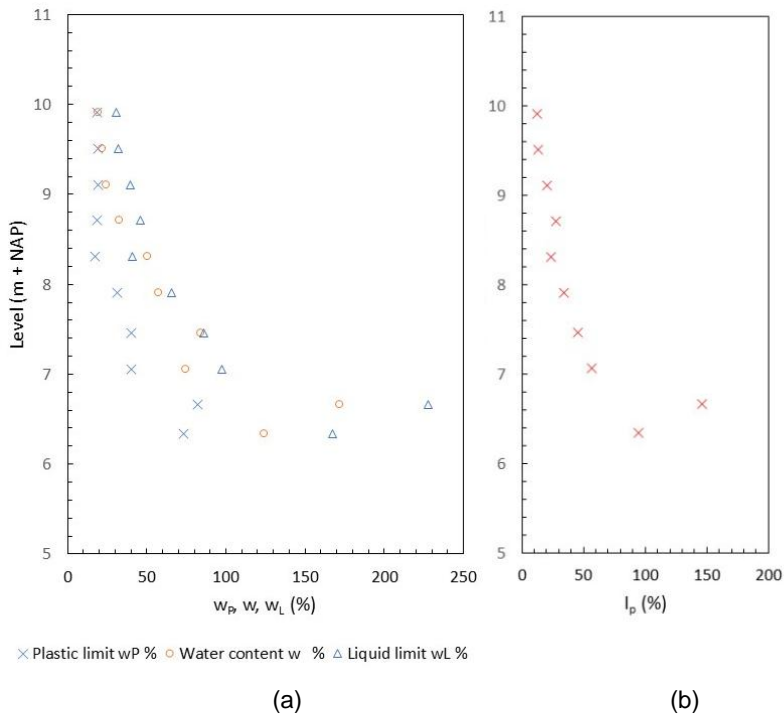


Figure 4.21 Profiles of (a) plastic limit  $w_P$ , liquid limit  $w_L$  and gravimetric water content  $w$  and (b) plasticity index  $I_p$  against depth from borehole B201 at Westervoort

The results of the classification tests as performed on the samples from borehole B001 at Oijen are summarized in Figure 4.22 – Figure 4.24.

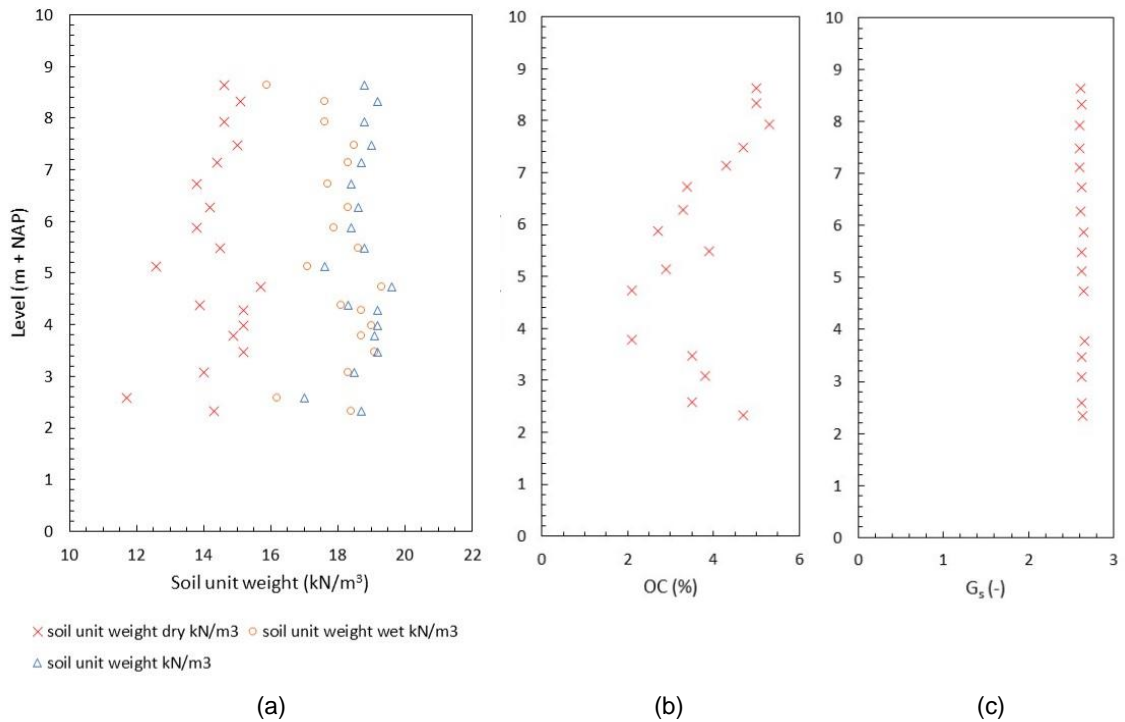


Figure 4.22 Profiles of (a) soil unit weight, (b) organic content (OC) and (c) specific gravity of the soil particles ( $G_s$ ) against depth from borehole B001 at Oijen

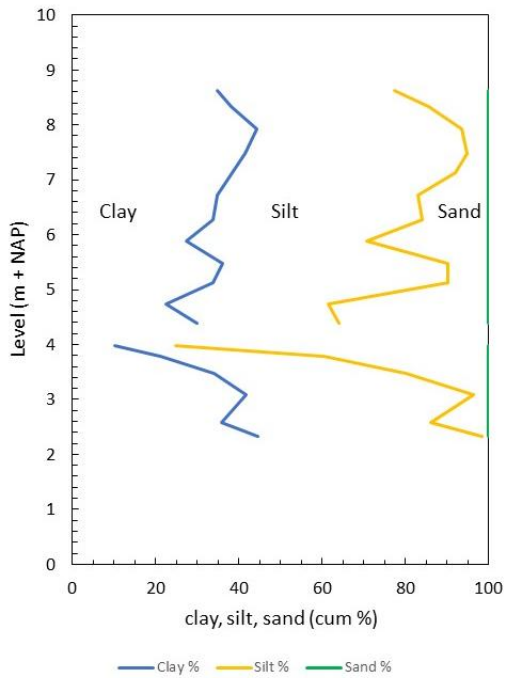


Figure 4.23 Profile of clay, silt and sand content against depth from borehole B001 at Oijen

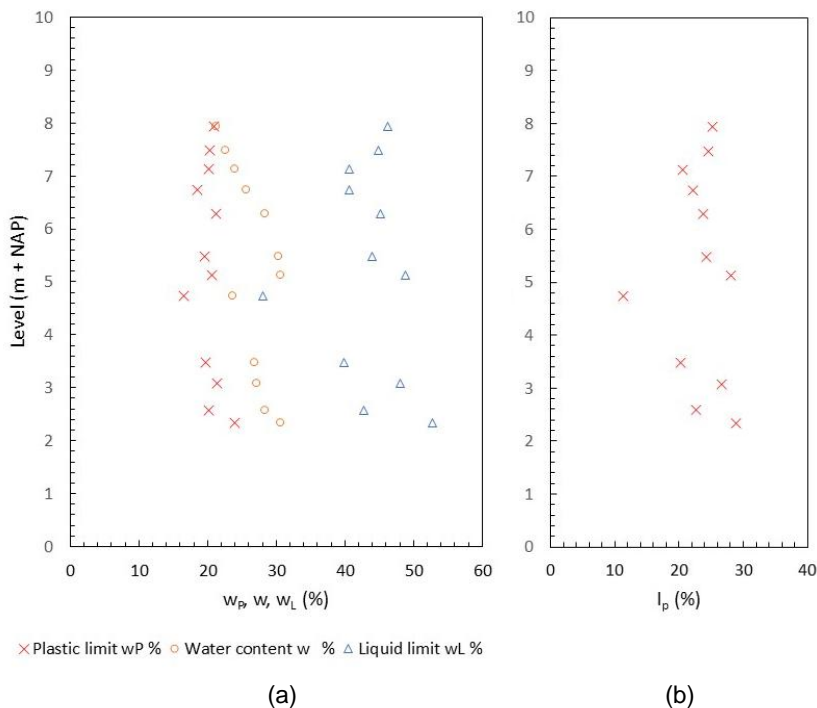


Figure 4.24 Profiles of (a) plastic limit  $w_P$ , liquid limit  $w_L$  and gravimetric water content  $w$  and (b) plasticity index  $I_p$  against depth from borehole B001 at Oijen

Specific surface of six intact clay samples and six reconstituted clay samples is determined using the  $N_2$  BET method. The results of these tests are presented in Table 4.1 and Table 4.2.

Location	Borehole	Sample	Level (NAP + m)	$\rho_{i,dry}$ (kg/m <sup>3</sup> )	Water content $w_i$ (-)	Specific surface S (m <sup>2</sup> /g)
Wester-voort	B203	15	9.79 – 9.66	1606	0.170	7.13
	B203	17	8.98 – 8.85	1541	0.264	22.10
	B203	21	7.82 – 7.64	999	0.619	19.90
Oijen	B003	3	8.38 – 8.26	1644	0.156	23.60
	B003	5	7.52 – 7.39	1534	0.254	20.80
	B003	11	4.97 – 4.85	1544	0.277	17.10

Table 4.1 Specific surface of intact samples determined with N<sub>2</sub> BET method

Sample	$\rho_{i,dry}$ (kg/m <sup>3</sup> )	Water content $w_i$ (-)	Water content $w_e$ (-)	Specific surface S (m <sup>2</sup> /g)
1	1533	0.250	0.234	10.8
3	1490	0.280	0.254	13.0
5	1589	0.200	0.238	14.5
8	1783	0.170	0.206	10.8
9	1472	0.300	0.298	11.3
11	1690	0.200	0.223	13.1

Table 4.2 Specific surface of reconstituted samples determined with N<sub>2</sub> BET method

#### 4.9 Determination of shear strength in the laboratory

The shear strength of intact and reconstituted samples is determined in the laboratory as described in Paragraph 3.10. On intact samples UU triaxial compression tests, direct simple shear tests and direct shear tests are performed. On reconstituted samples CIU triaxial compression tests are conducted. Results of UU triaxial compression tests on intact samples are presented in Table 4.3. Reports of the UU triaxial compression tests are in Appendix C.

Location	Bore-hole	Sample	Level (NAP + m)	$\rho_{i,dry}$ (kg/m <sup>3</sup> )	Water content $w_i$ (-)	$\sigma_v$ (kPa)	$t_{max}$ (kPa)	$t_{ult}$ (kPa)
Wester-voort	B203	15	9.79 – 9.66	1606	0.170	11.0	99,3	73
	B203	17	8.98 – 8.85	1541	0.264	25.7	56.3	56
	B203	21	7.82 – 7.64	999	0.619	45.2	20.4	17
Oijen	B003	3	8.38 – 8.26	1644	0.156	15.0	131.5	110
	B003	5	7.52 – 7.39	1534	0.254	31.1	86.7	80
	B003	11	4.97 – 4.85	1544	0.277	73.0	73.8	73.8

Table 4.3 Results of UU triaxial compression tests on intact samples

Other UU and CU triaxial compression tests are performed at TU Delft. The aim of these tests was to determine the relationship between water content, suction and shear strength. The results of these tests are reported in Appendix D. An example of the relationship between water content and shear strength is presented in Figure 4.25. Test T4 S2 (blue dot) gives the shear strength at fully saturated state. The relationship between water content and suction can be derived from soil water retention curves (see Paragraph 3.12 and Paragraph 4.11). Generally suction increases when water content decreases. So, the trend of increasing shear strength to decreasing water content in Figure 4.25 suggests that suction contributes to the shear strength in the UU triaxial tests.



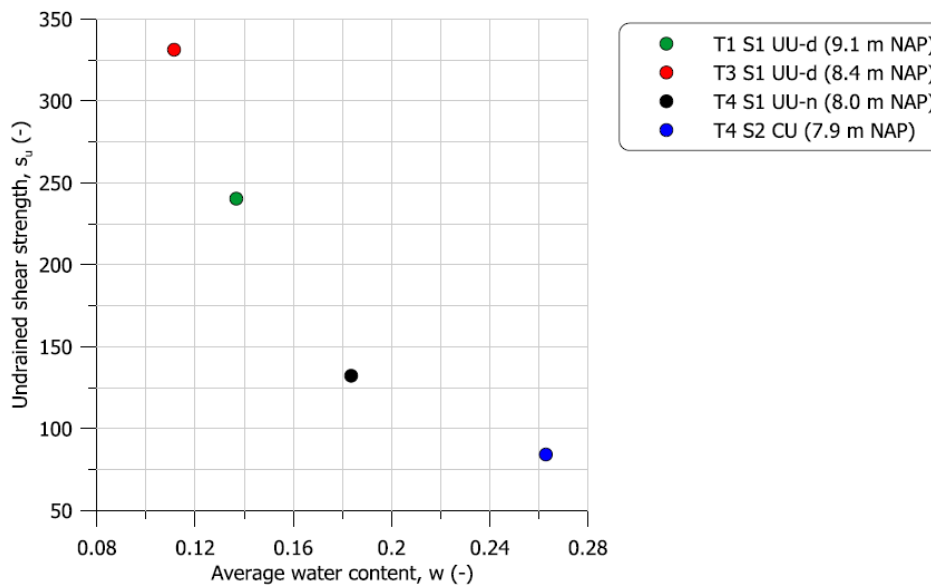


Figure 4.25 Relationship between water content and shear strength as derived from UU triaxial compression tests on intact samples (tests are performed at TU Delft)

Results of direct simple shear tests and direct shear tests on intact samples are given in Table 4.4. Reports of the direct simple shear tests and direct shear tests are in Appendix C.

Location	Bore-hole	Sample	Level (NAP + m)	$\rho_i$ (kg/m <sup>3</sup> )	Water content $w_i$ (-)	$\sigma_v$ (kPa)	$\tau_{max}$ (kPa)	$\tau_{ult}$ (kPa)
Westervoort	B203	14 (DS)	9.70 – 9.65	1790	0.132	11.0	68.9	19.0
	B203	16	8.85 – 8.80	1928	0.266	26.0	22.8	20.0
	B203	20	7.70 – 7.65	1650	0.607	44.1	25.5	25.3
Oijen	B003	2 (DS)	8.50 – 8.45	1608	0.137	9.0	102.1	77.3
	B003	4	7.25 – 7.20	1860	0.245	29.1	31.2	29.0
	B003	8	6.10 – 6.05	1940	0.256	51.1	34.3	33.0
	B003	10	5.02 – 5.00	1950	0.274	73.2	46.5	46.3

Table 4.4 Results of direct simple shear (DSS) tests and direct shear (DS) tests on intact samples

### Triaxial tests on reconstituted samples

As described in Paragraph 3.10 reconstituted samples are prepared in the laboratory and the shear strength of these samples is measured with CIU triaxial compression test. Table 4.5 gives the results of a series of tests on moist compacted samples. The samples are compacted using a standard Proctor hammer and Proctor mould according to ASTM D 698. The density “middle” with 25 blows per soil layer of 39 mm thickness corresponds to standard compaction effort following ASTM D 698. 67 mm diameter samples are used. After preparation the samples are saturated and consolidated to 50 kPa. An undrained shearing phase is applied. Reports of the CIU triaxial compression tests are in Appendix C.

Sample	Material preparation and compaction at water content $w_i$ (-)	Material compaction effort	$\rho_{i,bulk}$ (kg/m <sup>3</sup> )	$\rho_{i,dry}$ (kg/m <sup>3</sup> )	Water content $w_c$ (-)	$t_{max}$ (kPa)	$t_{ult}$ (kPa)
1	0.25	Loose (15 blows per soil layer of 39 mm thick)	1918	1533	0.234	50.4	50.4
2	0.17	Loose (idem)	1887	1617	0.252	47.3	47.3
3	0.28	Middle (25 blows per soil layer of 39 mm thick)	1902	1490	0.254	38.4	38.3
4	0.25	Middle (idem)	1919	1532	0.250	48.8	48.8
5	0.20	Middle (idem)	1906	1589	0.238	112.5	112.4
6	0.15	Middle (idem)	2009	1749	0.141	70.8	70.8
7	0.26	Dense (35 blows per soil layer of 39 mm thick)	1947	1551	0.232	51.5	51.5
8	0.17	Dense (idem)	2079	1783	0.206	194.9	194.9

Table 4.5 Results of CIU triaxial compression tests on reconstituted samples which are moist compacted using a Proctor hammer and Proctor mould with different compaction effort

A second series of reconstituted samples is prepared using the slurry method. The slurry is made applying a water content corresponding to 1.25 times the liquid limit  $w_L$ . The liquid limit of the intact samples which are used to prepare the reconstituted samples is between 0.3 and 0.5. The slurry samples are dried in the air to achieve different target water contents. 50 mm diameter samples are used to ensure that the time required for drying the samples became not too long. After preparation the samples are saturated and consolidated to 50 kPa. An undrained shearing phase is applied. Results of these tests are presented in Table 4.6. Reports of the CIU triaxial compression tests are in Appendix C.

Sample	Material dried in the air to target water content $w_i$ (-)	$\rho_{i,bulk}$ (kg/m <sup>3</sup> )	$\rho_{i,bulk}$ (kg/m <sup>3</sup> )	Water content $w_c$ (-)	$t_{max}$ (kPa)	$t_{ult}$ (kPa)
9	0.30	1912	1472	0.298	16.6	16.0
10	0.15	1949	1697	0.234	90.3	87.0
11	0.20	2019	1690	0.223	79.3	77.0
12	0.07	1876	1754	0.220	111.4	109.0
13	0.22	2010	1653	0.215	51.1	49.0

Table 4.6 Results of CIU triaxial compression tests on reconstituted samples which are made from a slurry and dried to different target water contents

### Oedometer tests

Oedometer tests are performed on intact samples and on a reconstituted sample. The intact samples are from boreholes B003 and B203. The reconstituted sample is a slurry sample from the same batch as the samples prepared for the triaxial tests. The test on the reconstituted sample (slurry) is performed to be able to compare the intrinsic soil behaviour with the behaviour of the intact samples. The properties of the tested samples are reported in Table 4.7. Reports of the oedometer tests are in Appendix C.

Location	Bore-hole	Sample	Level (NAP + m)	$\gamma_{i,bulk}$ (kN/m <sup>3</sup> )	$\gamma_{i,dry}$ (kN/m <sup>3</sup> )	Water content $w_i$ (-)
Westervoort	B203	13	9.65 – 9.60	17.6	15.6	0.128
	B203	19	7.65 – 7.60	16.2	10.2	0.586
Oijen	B003	1	8.45 – 8.40	16.2	14.0	0.153
	B003	7	6.05 – 6.00	19.2	15.5	0.237
	B003	7A	6.05 – 6.00	18.4	14.9	0.237

Table 4.7 Results of oedometer tests

### 4.10 Proctor test

The results of the Proctor test are given in Figure 4.26. The maximum dry density is 1673 kg/m<sup>3</sup> at optimum water content of 0.206.

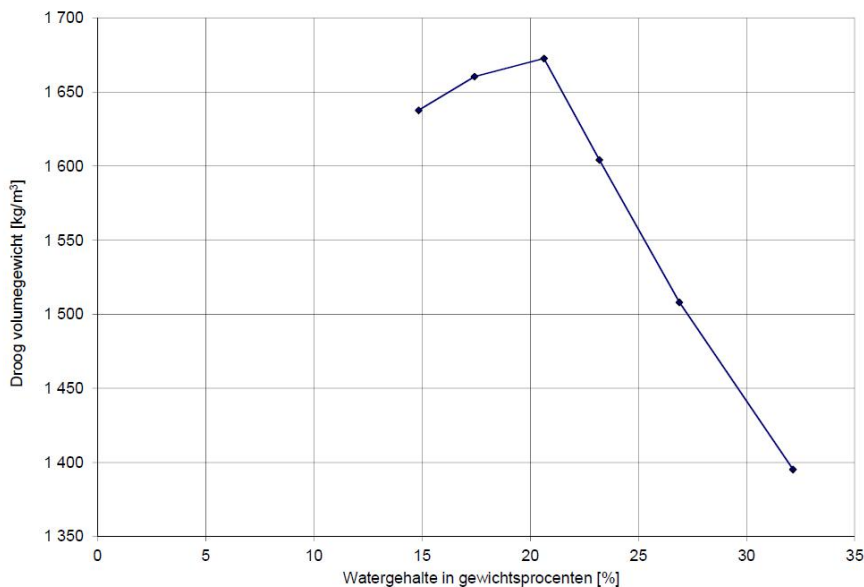


Figure 4.26 Results of the Proctor test

### 4.11 Determination of retention curves and shrinkage curves

The soil water retention curves as determined with the HYPROP tests at TU Delft are reported in Appendix D. An example of a HYPROP test, resulting in a soil water retention curve is given in Figure 4.27.

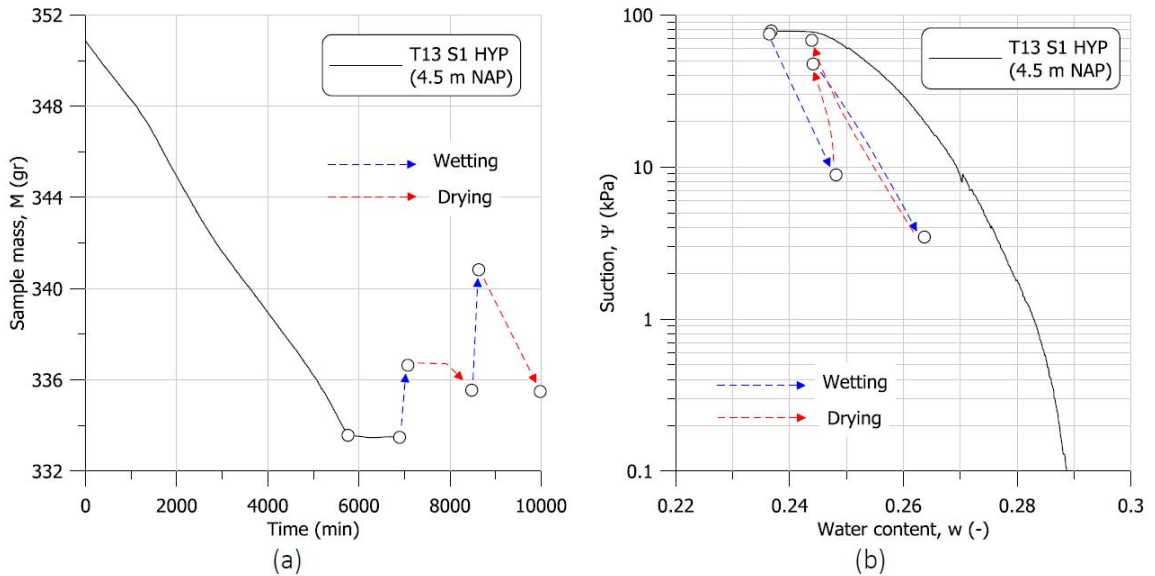


Figure 4.27 Example of HYPROP test resulting in a soil water retention curve

The relationship between water content and void ratio is measured in shrinkage tests. An example of a shrinkage test is depicted in Figure 4.28. The shrinkage tests are also performed at TU Delft. Results of the shrinkage tests are reported in Appendix D.

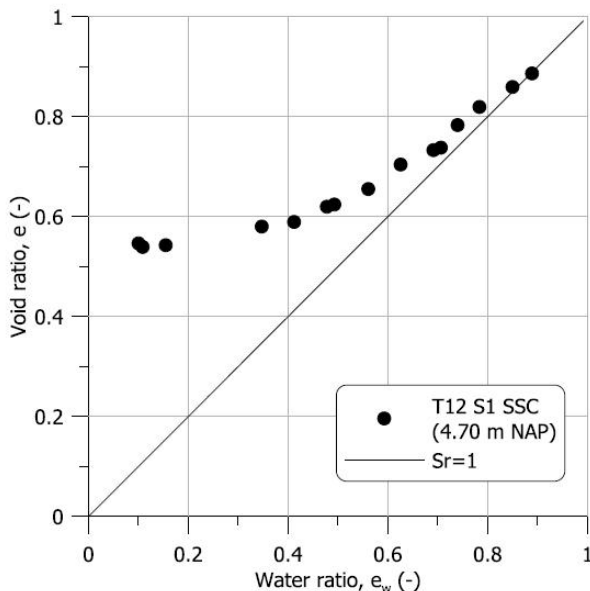


Figure 4.28 Example of shrinkage test

#### 4.12 Mercury intrusion porosimetry tests

The pore size distribution (PSD) of six intact clay samples and six reconstituted clay samples is determined using mercury intrusion porosimetry (MIP). The results of these tests are summarized in Table 4.8, Table 4.9 and Figure 4.29 and Figure 4.30. Figure 4.29 shows that the samples have a large number of pores with a size between 1 and 10  $\mu\text{m}$ . Water content of the samples increases with depth (see Table 4.8). Figure 4.29 shows that the modus of the PSD shift towards larger pore sizes with increasing depth and thus with increasing water

content. The results of the PSD of the reconstituted samples in Figure 4.30 are very similar to each other. Further study of these results is required to investigate what the effect of the samples preparation on the PSD is.

Location	Borehole	Sample	Level (NAP + m)	$\rho_{i,dry}$ (kg/m <sup>3</sup> )	Water content (-)
Westervoort	B203	15	9.79 – 9.66	1606	0.170
	B203	17	8.98 – 8.85	1541	0.264
	B203	21	7.82 – 7.64	999	0.619
Oijen	B003	3	8.38 – 8.26	1644	0.156
	B003	5	7.52 – 7.39	1534	0.254
	B003	11	4.97 – 4.85	1544	0.277

Table 4.8 Intact clay samples for the determination of the pore size distribution

Sample	$\rho_{i,dry}$ (kg/m <sup>3</sup> )	Water content $w_i$ (-)	Water content $w_e$ (-)
1	1533	0.250	0.234
3	1490	0.280	0.254
5	1589	0.200	0.238
8	1783	0.170	0.206
9	1472	0.300	0.298
11	1690	0.200	0.223

Table 4.9 Reconstituted clay samples for the determination of the pore size distribution

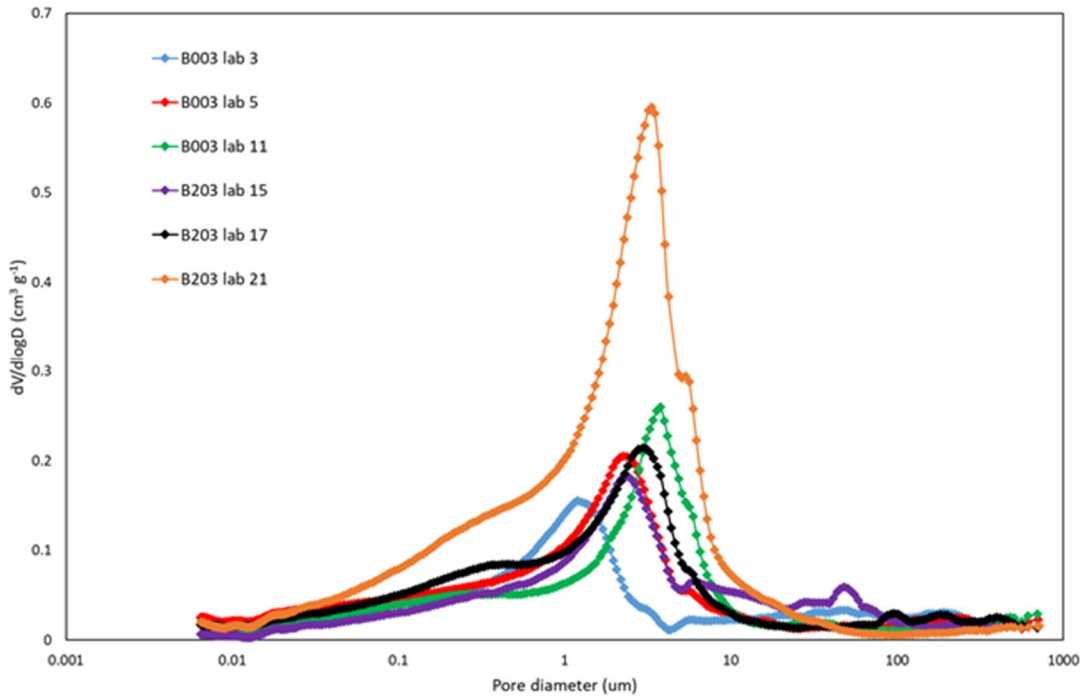


Figure 4.29 Pore size distribution from six intact clay samples determined with mercury intrusion porosimetry

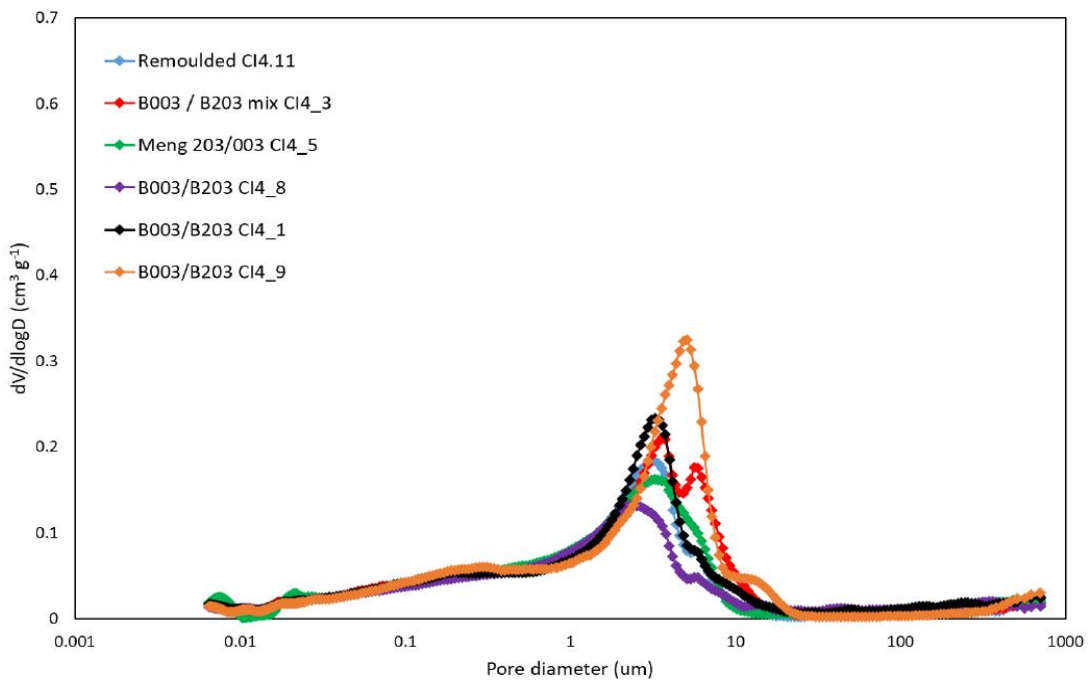


Figure 4.30 Pore size distribution from six reconstituted clay samples determined with mercury intrusion porosimetry

## 5 Summary

This report describes the methods and some preliminary results of the research of the shear strength of initially unsaturated soils at the IJsseldijk near Westervoort (Dp. 250 + 80) and Maasdijk near Oijen (Dp. 592 - 593). The research concerns monitoring of volumetric water content, suction and pore water pressure and the measurements of the in-situ shear strength with cone penetration tests and field vane tests. Boreholes, classification tests and various tests to measure the shear strength in the laboratory are also conducted. Volumetric water content and suction will be related to the measurements of the shear strength in order to quantify the influence of the volumetric water content and suction on the shear strength.

The present results of the period October 2019 – November 2020 show a seasonal variation of volumetric water content, suction and shear strength. In the second part of the winter the shear strength is relatively low; with a minimum shear strength around 30 kPa or more. In this period suction is also very low. In spring shear strength increases. High shear strength values can be measured at shallow depth. In summer the shear strength also increases at larger depth, but due to precipitation the shear strength near surface level can be lower compared to spring. In summer suction can be above 80 kPa in the first meters below surface level. Notwithstanding the variations of suction and the shear strength the measured shear strength is at both locations still substantially higher (four to five times higher on average) than the drained shear strength based on the friction angle  $\phi'$ . Laboratory tests are performed to investigate different effects which may have an effect on the minimum strength which can be mobilized in winter despite the measured suction is negligible.

Note that this report describes only preliminary measurement results. A more elaborate interpretation of the data, including the results of the laboratory tests, has to be performed. At Oijen no significant high-water level occurred which could have influenced the water content, suction and density of the clay in the dyke body. Therefore, one has to be cautious to apply these preliminary results in the assessments of dykes and to translate the preliminary results to other cases. A longer measurement period and measurements at other locations are required to get more insight in the processes and possible variations in the shear strength due to more extreme conditions.

The measurements at Westervoort and Oijen will be continued in 2021 in order to be able to monitor volumetric water content, suction and shear strength in the different seasons with different amounts of precipitation and evaporation. These new results from the field tests will be added to the next versions of this report.

## 6 References

- Akin, I. D., & Likos, W. J. (2014). Specific surface area of clay using water vapor and EGME sorption methods. *Geotechnical Testing Journal*, 37(6), 1016-1027.
- Arnepalli, D. N., Shanthakumar, S., Rao, B. H., & Singh, D. N. (2008). Comparison of methods for determining specific-surface area of fine-grained soils. *Geotechnical and Geological Engineering*, 26(2), 121-132.
- ASTM D 698. (2000). Standard test method for laboratory compaction characteristics of soil using standard effort. Easton, PA: American Society for Testing and Materials.
- ASTM. D2573-01. (2008). Standard test method for field vane shear test in cohesive soil. ASTM West Conshohocken, PA.
- ASTM. D 3080. (1994). Standard test method for Direct Shear Test of soils under consolidated drained conditions. (Withdrawn 2020, no replacement). ASTM West Conshohocken, PA.
- ASTM D 4404-18. Standard Test Method for Determination of Pore Volume and Pore Volume Distribution of Soil and Rock by Mercury Intrusion Porosimetry.
- ASTM. D 6528. (2007). Standard Test Method for Consolidated Undrained Direct Simple Shear Testing of Cohesive Soils. ASTM West Conshohocken, PA.
- Azzouz, A. S., Baligh, M. M., & Ladd, C. C. (1983). Corrected field vane strength for embankment design. *Journal of Geotechnical Engineering*, 109(5), 730-734.
- Becker, D. E., Crooks, J. H., & Been, K. (1988). Interpretation of the Field Vane Test in Terms of In-Situ and Yield Stresses in Vane Shear Strength Testing in Soils. *Field and Laboratory Studies*, Richards, AF, Editor, ASTM, 71-87.
- Bjerrum, L. (1972). Embankments on Soft Ground, State-of-the-Art Report, presented at the June 11-14, ASCE Specialty Conference on Performance of Earth and Earth-Supported Structures, held at Lafayette, Ind., Vol. 2, pp. 1-54.
- Bjerrum, L. (1973). Problems of soil mechanics and construction on soft clays and structurally unstable soils. In *Proc. 8th ICSMFE* (Vol. 3, pp. 111-159).
- Blight, G. (2013). *Unsaturated Soil Mechanics in Geotechnical Practice*. Leiden, The Netherlands: CRC Press/Balkema.
- Brunauer, S., Emmett, P. H., & Teller, E. (1938). Adsorption of gases in multimolecular layers. *Journal of the American chemical society*, 60(2), 309-319.
- Campbell. (2016). CS616 and CS625 Water Content Reflectometers. Instruction manual. Revision 2/16. Campbell Scientific, Inc.
- Chandler, R. J. (1988). The in-situ measurement of the undrained shear strength of clays using the field vane. In *Vane shear strength testing in soils: field and laboratory studies*. ASTM International.
- Deltares. (2016). Protocol laboratoriumproeven voor grondonderzoek aan waterkeringen. Deltares rapport 1230090-019-GEO-0002, Versie 03, 25 mei 2016, definitief.
- Deltares. (2019a). Shear Strength of Initially Unsaturated Soil - Literature Study and Research Proposal. Deltares report 11202560-020-GEO-0001, January 16, 2019.
- Deltares. (2019b). Plan van Aanpak KPP 2019 project - WK01 2019 - Kennis voor Keringen.
- Deltares. (2019c). Plan van aanpak onderzoek schuifsterkte (initieel) onverzadigde grond. 11204453-000-GEO-0001. 27 augustus 2019.
- Deltares. (2019d). Verkenning Diëlektrische Sondeer Conus GeoPoint.
- FprEN 22476-9:2010.3 (E) (CEN/TC 341 date: 2010-12): Ground investigation and testing - Field testing -Part 9: Field vane test.
- Geokon. (2019). VW Piezometers & Pressure Transducers. 4500 Series.
- Grondmechanica Delft. (1996). Onderzoek stabiliteit Maasdijken, Vak D, Oijen Benedeneind – Zuiveringsinstal. HM 574 tot HM 595. Geotechnisch Profiel G-G'. Project CO-361580.



- Inpijn-Blokpoel. (2017). Grondonderzoek voor de 4e toetsronde - Resultaten geotechnisch onderzoek. Documentnummer 02P008040-RG-01. 1 augustus 2017.
- ISO 15901-1:2016. Evaluation of pore size distribution and porosity of solid materials by mercury porosimetry and gas adsorption – Part 1: Mercury porosimetry.
- ISO 17892-8:2018. Geotechnical investigation and testing — Laboratory testing of soil — Part 8: Unconsolidated undrained triaxial test.
- Koliji, A., Vulliet, L., & Laloui, L. (2010). Structural characterization of unsaturated aggregated soil. *Canadian Geotechnical Journal*, 47(3), 297-311.
- Ladd, C. C., & DeGroot, D. J. (2004). Recommended practice for soft ground site characterization: Arthur Casagrande Lecture, 12th Panam. In *Conf. on Soil Mechanics and Geotechnical Engineering*.
- Larsson, R., Bergdahl, U., & Eriksson, L. (1987). Evaluation of shear strength in cohesive soils with special reference to Swedish practice and experience. *Geotechnical Testing Journal*, 10(3), 105-112.
- Larsson, R., & Åhnberg, H. (2005). On the evaluation of undrained shear strength and preconsolidation pressure from common field tests in clay. *Canadian geotechnical journal*, 42(4), 1221-1231.
- Liu, X., Buzzi, O., Yuan, S., Mendes, J., & Fityus, S. (2016). Multi-scale characterization of retention and shrinkage behaviour of four Australian clayey soils. *Canadian Geotechnical Journal*, 53(5), 854-870.
- Lu, Q., Randolph, M. F., Hu, Y. & Bugarski, I. C. (2004). A numerical study of cone penetration in clay. *Géotechnique* 54, No. 4, pp. 257–267.
- Mayne, P. (2007). *Cone Penetration Testing*. Washington: Transportation Research Board.
- Meter. (2018). T5/T5x Pressure Transducer Tensiometer - User Manual. METER Group AG München. Art. Nr. T5. Version 08/2018.
- Miller, G. A., Collins, R. W., Muraleetharan, K. K., Cerato, A. B., & Doumet, R. (2015). Interpretation of in situ tests as affected by soil suction, Report FHWA-OK-15-09. Oklahoma Department of Transportation.
- Ministerie van Infrastructuur en Milieu. (2019). Schematiseringshandleiding Macrostabiliteit, WBI 2017, 28 november 2019, definitief, versie 3.0.
- Mitchell, J. K., & Soga, K. (2005). *Fundamentals of soil behavior* (Vol. 3). New York: John Wiley & Sons.
- NEN-EN-ISO 14688-2, Geotechnisch onderzoek en beproeving - Identificatie en classificatie van grond - Deel 2: Grondslagen voor een classificatie.
- NEN-EN-ISO 17892-1, Geotechnisch onderzoek en beproeving - Beproeving van grond in het laboratorium - Deel 1: Bepaling van het watergehalte.
- NEN-EN-ISO 17892-2, Geotechnisch onderzoek en beproeving - Beproeving van grond in het laboratorium - Deel 2: Bepaling van de dichtheid van fijn korrelige grond.
- NEN-EN-ISO 17892-3, Geotechnisch onderzoek en beproeving - Beproeving van grond in het laboratorium - Deel 3: Bepaling van de dichtheid van gronddeeltjes.
- NEN-EN-ISO 17892-4, Geotechnisch onderzoek en beproeving - Beproeving van grond in het laboratorium - Deel 4: Bepaling van de korrelgrootte verdeling.
- NEN-EN-ISO 17892-5:2017 en. Geotechnical investigation and testing - Laboratory testing of soil - Part 5: Incremental loading oedometer test.
- NEN-EN-ISO 17892-9:2018 en. Geotechnical investigation and testing - Laboratory testing of soil - Part 9: Consolidated triaxial compression tests on water saturated soils.
- NEN-EN-ISO 17892-12, Geotechnisch onderzoek en beproeving - Beproeving van grond in het laboratorium - Deel 12: Bepaling van de Atterbergse grenzen.
- NEN-EN-ISO 22475-1, Geotechnisch onderzoek en beproeving - Methoden voor monsterneming en grondwatermeting - Deel 1: Technische grondslagen voor de uitvoering.

- NEN-EN-ISO 22476-1. (2013). Geotechnisch onderzoek en beproeving – Veldproeven – Deel 1: Elektrische sondering. Nederlands Normalisatie Instituut.
- Pournaghiazar, M., Russell, A., & Khalili, N. (2013). The cone penetration test in unsaturated sands. *Géotechnique*, 63, No. 14, 1209–1220.
- Powell, J., & Quarterman, R. (1988). The interpretation of cone penetration tests in clays, with particular reference to rate effects. 1st Int. Symp. on Penetration Testing, (pp. 903-909). Orlando, USA.
- Romero, E., & Simms, P. H. (2008). Microstructure investigation in unsaturated soils: a review with special attention to contribution of mercury intrusion porosimetry and environmental scanning electron microscopy. *Geotechnical and Geological engineering*, 26(6), 705-727.
- Santamarina, J. C., Klein, K. A., Wang, Y. H., & Prencke, E. (2002). Specific surface: determination and relevance. *Canadian Geotechnical Journal*, 39(1), 233-241.
- Schnaid, F. (2009). *In Situ Testing in Geomechanics*. Oxon: Taylor & Francis.
- SIKB. (2018). Protocol 2101. Mechanisch boren. BRL SIKB 2100.
- Tarantino, A., Ridley, A., & Toll, D. (2008). Field Measurements of Suction, Water Content, and Water Permeability. *Geotech. Geol. Eng.*, 751-782.
- Teh, C. I. & Houlsby, G. T. (1988). Analysis of the cone penetration test by the strain path method. In: *Numerical Methods in Geomechanics*. Innsbruck. Swoboda (ed.). Balkema, Rotterdam.
- UGT. (2020). Full Range Tensiometer. Operating Manual. Version: 20/07/20.



## **A Results of in situ tests and classification tests of location Westervoort (in Dutch)**

Geotechnisch onderzoek - Meetlocatie IJsseldijk te Westervoort  
Rapport VN-74499-1 | 19 november 2020  
Wiertsema & Partners



## **B Results of in situ tests and classification tests of location Oijen (in Dutch)**

Geotechnisch onderzoek - Meetlocatie Maasdijk te Oijen  
Rapport VN-74499-1 | 19 november 2020  
Wiertsema & Partners

## **C Results of laboratory tests on intact and reconstituted samples of locations Oijen and Westervoort**

## **D Results of triaxial tests and HYPROP tests on intact samples of locations Westervoort and Oijen**

Shear Strength of Initially Unsaturated Soil  
Laboratory results  
Revision 1  
Date 21 October 2020  
TU Delft



## **E Results of mercury intrusion porosimetry (MIP) tests and determination of specific surface on intact samples of locations Westervoort and Oijen**

Delft Solids Solutions  
Report 20-DSS-0868  
16 December 2020